

**Accounting for extinction dynamics unifies the geological and biological histories of Indo-Australian Archipelago**

Herrera-Alsina, Leonel; Lancaster, Lesley T; Algar, Adam C; Bocedi, Greta; Papadopoulos, Alexander S T; Gubry-Rangin, Cecile; Osborne, Owen G; Mynard, Poppy; Creer, Simon; Villegas-Patracca, Rafael; Made Suidiana, I; Fahri, Fahri; Lupiyaningdyah, Pungki; Nangoy, Meis; Iskandar, Djoko T; Juliandi, Berry; Burslem, David F R P; Travis, Justin M J

Proceedings of the Royal Society B: Biological Sciences

DOI:

[10.1098/rspb.2024.0966](https://doi.org/10.1098/rspb.2024.0966)

E-pub ahead of print: 30/09/2024

Peer reviewed version

[Cyswllt i'r cyhoeddiad / Link to publication](#)

Dyfyniad o'r fersiwn a gyhoeddwyd / Citation for published version (APA):

Herrera-Alsina, L., Lancaster, L. T., Algar, A. C., Bocedi, G., Papadopoulos, A. S. T., Gubry-Rangin, C., Osborne, O. G., Mynard, P., Creer, S., Villegas-Patracca, R., Made Suidiana, I., Fahri, F., Lupiyaningdyah, P., Nangoy, M., Iskandar, D. T., Juliandi, B., Burslem, D. F. R. P., & Travis, J. M. J. (2024). Accounting for extinction dynamics unifies the geological and biological histories of Indo-Australian Archipelago. *Proceedings of the Royal Society B: Biological Sciences*, 291(2031), 20240966. Advance online publication. <https://doi.org/10.1098/rspb.2024.0966>

Hawliau Cyffredinol / General rights

Copyright and moral rights for the publications made accessible in the public portal are retained by the authors and/or other copyright owners and it is a condition of accessing publications that users recognise and abide by the legal requirements associated with these rights.

- Users may download and print one copy of any publication from the public portal for the purpose of private study or research.
- You may not further distribute the material or use it for any profit-making activity or commercial gain
- You may freely distribute the URL identifying the publication in the public portal ?

Take down policy

If you believe that this document breaches copyright please contact us providing details, and we will remove access to the work immediately and investigate your claim.

53 Introduction

54

55 The surface of our planet has been altered greatly on geological timescales, which
56 has impacted the diversity of life at the highest level: many species are created and
57 go extinct at the tempo of major geological events. Our ability to reconstruct the
58 evolution of global biodiversity can therefore be achieved only by combining
59 evidence from geology and biogeography. The Indo-Australian Archipelago (IAA)
60 provides a prime example of this principle, because its striking biodiversity can only
61 be understood by its geological dynamism (Carter et al., 2001; Zahirovic et al.,
62 2014). The modelled geological history of IAA has critically influenced the
63 biogeographic modelling of diverse clades (ranging from plants to vertebrates) and
64 vice versa. However, new geological evidence has created a mismatch between
65 biogeographic patterns and the connectivity of the landmasses in the region. Here,
66 we aim to resolve this paradox by modelling and incorporating a key evolutionary
67 process, species extinction, into biogeographic reconstructions.

68 The spatial configuration of islands and continental landmasses across IAA has
69 changed considerably over geological timescales. There is a long-standing paradigm
70 proposing that the Malay peninsula and Greater Sunda islands were totally
71 disconnected from (at least) 60 Ma (Lohman et al., 2011) to 10 Ma, when the
72 appearance of the islands now forming the Indonesian archipelago and Wallacea
73 region could have served as stepping-stones for the dispersal of some clades. This
74 geological hypothesis was supported by evolutionary studies conducted using
75 modern geographic distributions and phylogenetic trees of extant species, which
76 appeared to find constrained dispersal in ancient lineages across IAA, due to an
77 extensive period when islands were not connected. Both animal (Dong et al., 2018)
78 and plant (Nauheimer et al., 2012; Williams et al., 2017) lineages that arose as early
79 as 40 Ma underwent limited dispersal within but not between their centres of origin
80 on either the Sunda or Sahul continental shelf, before dispersing elsewhere. Other
81 taxonomic groups are documented to have originated in the Indochina peninsula,
82 with a further dispersal eastward to colonize New Guinea (Atkins et al., 2020;
83 Grudinski et al., 2014), while the Philippines are thought to have been colonised
84 relatively recently (Thomas et al., 2012). Other clades seem to have originated in the
85 eastern part of the region followed by subsequent colonization events towards
86 continental Asia (Bocek & Bocak, 2019). Consistent with the idea of limited dispersal
87 across the archipelago, widespread species are likely to form new species that
88 become endemic to individual islands (Simaiakis et al., 2012). The fundamental role
89 of this mechanism is reflected in high rates of vicariance (i.e., speciation due to
90 differentiation between two populations which that different islands). Under this view,
91 dispersal facilitation by the late appearance of island steppingstones is common to
92 the biogeographical reconstructions of all the lineages that have been examined in
93 recent studies (Atkins et al., 2020; Thomas et al., 2012).

94 Many studies have applied standard biogeographic reconstruction methods and
95 weaved biogeographical hypotheses that are consistent with this geological
96 hypothesis. However, this understanding of the geological history of IAA has recently
97 been challenged by geomorphological evidence pointing to the presence of ancient
98 land bridges between mainland Asia and the Indonesian islands (Husson et al.,
99 2020; Salles et al., 2021; Sarr et al., 2019). For instance, it is hypothesized that
100 Sundaland (i.e., the western part of the archipelago) was permanently continental

101 until at least 6 Ma (Husson et al., 2020), which pre-dates the onset of regional
102 connectivity by tens of millions of years (Hall, 2013). This hypothesis conflicts with
103 the patterns seen in current reconstructions of biogeography for the region (Atkins et
104 al., 2020; Dong et al., 2018; Su & Saunders, 2009). There is thus a mismatch
105 between interpretations of the region's history from the perspectives of geological
106 and biological evidence.

107 One potential explanation for this disparity is that inferring the true biogeographic
108 histories of clades is complicated by unrecorded species extinctions. Extinction
109 inevitably removes the evidence of geographic distributions of extinct species in
110 reconstructed phylogenetic trees. Traditional biogeographic approaches model only
111 *local* extinction (also known as extirpation), which is different from lineage/species
112 extinction. Recent work has demonstrated that two clades with the same history of
113 speciation and rates of range evolution (i.e., colonization and local extirpation), can
114 be inferred erroneously to have different origins and historical biogeographical
115 dispersal events if they differ in background rates of lineage extinction (Herrera-
116 Alsina et al., 2022). Thus, radically different biogeographical reconstructions of
117 regional biotas can be inferred when extinct lineages and their distributions are
118 modelled explicitly. The amount of historical extinction in IAA is unknown but is likely
119 to be high (Louys et al., 2007). A discordance between current geological
120 understanding of the region's history and our best biological understanding might
121 arise because lineage extinctions have not been accounted for in previous
122 biogeographic inferences.

123 Specifically, we hypothesize that clades used land bridges connecting the major IAA
124 landmasses since their origin. If that is the case, we expect to find evidence against
125 limitation in ancient dispersal, wider ancient geographic distributions and early
126 colonization of the entire archipelago (compared to zero-extinction models).
127 Furthermore, we expect that high connectivity among landmasses limits geographic
128 isolation, which in turn decreases the likelihood of differentiation among allopatric
129 populations (i.e., inhabiting different islands) leading to vicariant speciation,
130 compared to in-situ speciation (i.e., speciation within an island or location through
131 any potential mechanism including fine-scale geographic isolation).

132 To test this hypothesis, we revisited the biogeographic history of clades that had
133 been used previously to characterize the patterns of speciation and dispersal in IAA.
134 These clades differ in their dispersal capacities and life histories, possess high-
135 quality phylogenetic trees and well-known geographic distributions. We collated data
136 used to reconstruct the phylogenies and biogeographic histories of eight clades
137 representing plants, invertebrates and vertebrates (the breadfruits *Artocarpus*,
138 orchids *Paphiopedilum*, treelets *Pseuduvaria*, taros *Alocasia*, crabs *Parathelphusa*,
139 crickets *Cardiodactylus*, parachuting frogs *Rhacophorus*, and herbs *Cyrtandra*) that
140 have diversified across IAA over the last 45 million years. We considered the
141 influence of extinction on the biogeographic reconstructions by explicitly modelling
142 both the missing branches (due to extinction) on a phylogenetic tree and the
143 geographic distribution of those extinct lineages. Our approach uses contemporary
144 species distributions and does not require paleogeographic information. We applied
145 a likelihood framework where tree branches are used to compute the change in
146 probability of a lineage (extant) being present at a given location. This probability

147 also considers that a lineage could have existed at any point along a branch, could
148 have changed across locations, and went extinct before the present.

149

150 Results

151 By explicitly accounting for lineage extinctions, we obtain substantially different
152 geographic origins and patterns of species distributions on the biogeographical
153 histories of clades in the Indo-Australian Archipelago to that inferred from models
154 assuming zero extinction. When extinction is included, we find much greater
155 concordance between the clades' geographic origins (Fig. 1), we infer much earlier
156 spread across the region for all clades (Fig. 2) and we find that in-situ speciation
157 becomes more important relative to vicariant speciation in generating the
158 contemporary biodiversity of the region (Fig. 3).

159 *A cradle for clades*

160 When we set our models to assume zero extinction, we recovered the same
161 geographic origins as those reported in the original studies. Models with zero
162 extinction showed that all eight clades had narrow geographic origins that, in
163 general, included either continental Asia or New Guinea. We found that the inferred
164 geographic origin of the common ancestor of a clade changed when extinction rates
165 higher than zero were assumed in the models. For instance, in *Cardiodactylus*
166 crickets, a model assuming zero extinction reconstructs New Guinea as the original
167 ancestral range, but when extinction was allowed, Borneo and continental Asia were
168 inferred to be the centre of origin. In all cases apart from *Cyrtandra* herbs we found
169 that Borneo and continental Asia were included within the centre of origin when
170 extinction was explicitly incorporated into models (Fig. 1).

171 *Dispersal and early land connectivity in IAA*

172 We estimated substantially earlier dates at which clades arrived onto different
173 landmasses when models assumed lineage extinction rates higher than zero than
174 when extinction was neglected (Fig. 1). For example, the breadfruit (*Artocarpus*)
175 clade is predicated to have colonized the Philippines earlier in its evolution (22 Mya
176 versus 10 Mya as previously estimated; Fig. 1); for taros (*Alocasia*), Sulawesi is
177 estimated to have been colonized much earlier in models assuming
178 intermediate/high extinction rates (35 Ma), than in models with zero extinction (7
179 Ma). For *Cyrtandra* herbs, the expansion out of Borneo is estimated to have occurred
180 at least 2 million years earlier than previously thought; Sumatra, for instance, is
181 estimated to have been part of the geographic range of *Cyrtandra* for the last 10.5
182 million years, whereas models assuming no extinction infer colonization of Sumatra
183 only 6 Mya. Sulawesi is the location that shows more differences.

184 *Mechanisms of speciation and species accumulation*

185 Our revised models incorporating non-zero extinction reconstruct different patterns in
186 the distribution of species diversity across IAA over time than zero-extinction models.
187 For instance, the Philippines are estimated to have accumulated breadfruit species
188 (*Artocarpus*) soon after colonization by the genus in the late Eocene (Fig. 2). Another
189 interesting finding is that Borneo was richer in *Paphiopedilum* orchid species at 20
190 Mya than it is at the present. Because our models assume a constant rate of
191 extirpation over time, the reduction in orchid species in Borneo is not associated with
192 increased rate of extirpation. Instead, the decreasing orchid richness is caused by
193 [global] processes that led to lineage extinction (Wilting et al., 2012). The low
194 extinction scenario reconstructs Sulawesi to have low species richness through time
195 (Fig 2), in contrast with the high extinction case where Sulawesi harbours high

196 diversity since the Eocene (Figures S25, S26). Sulawesi is the location that shows
197 more striking differences in how diversity accumulated over time across the different
198 scenarios of species extinction. Taken together, these new reconstructions of the
199 biogeographic histories of the eight clades provide a substantially altered picture of
200 much earlier accumulation of species diversity and richness across IAA and much
201 less certainty on the inference that these taxa had spatially disparate origins (Fig. 2,
202 Fig. S1-S24).

203 We find that the relative contribution of vicariance and in-situ speciation also
204 depends on the assumed extinction rate, and that this contribution varies across
205 taxonomic groups. The contribution of in-situ speciation increases with the assumed
206 rate of lineage extinction. When lineage extinction is assumed to be low, vicariance
207 is estimated to be higher than in-situ speciation, except in breadfruits and
208 parachuting frogs where in-situ speciation is the main mechanism of speciation. By
209 increasing extinction to a more realistic intermediate rate, our analysis shows that in
210 situ speciation also dominates for *Pseuduvaria treelets* and taros (Fig. 3). For the
211 models assuming high rates of extinction, in-situ speciation is the main mechanism
212 behind diversification in all groups. When varying the assumed rates of extinction,
213 the model does not compensate for changes in ancestral distributions by fitting high
214 rates of range evolution. Instead, the estimated rates of range evolution are similar
215 across different extinction rates, which demonstrates that our model successfully
216 disentangles species extinction from extirpation (i.e., local extinctions).

217

218

219 Discussion

220 Our results suggest that the eight biological radiations in the Indonesian Archipelago
221 we analysed are characterized by early and widespread dispersal which results in a
222 reconstructed widespread distribution of the common ancestor. We found that all
223 clades were present within the landmasses represented by all the modern islands far
224 earlier than was previously thought, and that expansion across the region generally
225 occurred soon after the rise of a taxonomic group. As we included groups with large
226 differences in dispersal capacities and evolutionary age, our results suggest that the
227 movement of species throughout the region was not strongly constrained and that a
228 large part of IAA might have been connected by islands or island-like land bridges
229 for an extended period over the past 45My. Importantly, it was necessary to account
230 for species extinctions during lineage evolution to uncover these patterns. Under this
231 scenario, vicariance processes are less likely to explain diversification, but instead,
232 speciation events take place within the areas that now form the major islands of
233 contemporary Southeast Asia.

234 By modelling extinction, we found that ancient dispersal of lineages across Indo-
235 Australian Archipelago (IAA) took place much earlier than estimated by previous
236 studies. Even though our conclusions are based on eight clades, they are congruent
237 with recent geomorphological information (Husson et al. 2020) and fossil evidence.
238 Fossil ostracods (Crustacea) have been found in the region of modern Java, and
239 importantly, their subtidal lifestyle (based on eye tubercle morphology) suggests that
240 land was available around 40- 38 MA (Yasuhara et al., 2017). The palynological
241 record shows that mangroves were already inhabiting Sumatra during the Middle
242 Eocene (~ 40-45 MA; Ellison et al., 1999; Renema et al., 2008). Because mangroves

243 occur at the interface between terrestrial and marine environments, this fossilized
244 pollen also provides evidence of the presence of landmasses in the region at this
245 time. These findings are incongruent with zero extinction biogeographic
246 reconstructions that typically conclude more recent colonisation across the region,
247 and they suggest that elevated rates of background extinction are required for
248 accurate biogeographical reconstruction of the region. This conclusion is supported
249 by climatic factors suggesting that lineage extinction is likely to be high in this region
250 (Louys et al., 2007).

251 Our models consistently selected Borneo and continental Asia (plus New Guinea
252 and Sumatra for three groups, the Philippines for two and Sulawesi once) as the
253 geographic origin of the eight clades. The modelled taxonomic groups do not only
254 differ in life history traits but also greatly vary in their evolutionary age, which
255 suggests that the former landmass represented by these territories has consistently
256 played an important role in shaping the biota of IAA (De Bruyn et al., 2014).
257 Sundaland has been the cradle of entire taxonomic groups and also the stage of
258 many speciation events, reinforcing its role as an evolutionary source of biodiversity,
259 rather than the destination (De Bruyn et al., 2014; Grismer et al., 2016). For
260 instance, the reconstructed common ancestor of *Cardiodactylus* crickets, which was
261 previously thought to be of Sahul origin, is now shown to be present in Sundaland.
262 When intermediate and high rates of extinction were assumed, our models suggest
263 that continental Asia and Borneo have been occupied by all eight clades throughout
264 their history.

265 Our results suggest that the estimate of the relative contributions of in-situ and
266 vicariant speciation change when varying the assumed extinction rate. Models
267 featuring high extinction rates estimate that, on average, in-situ speciation is higher
268 than vicariant speciation. There are two potential reasons for this. On the one hand,
269 vicariance can take place only when species are geographically widespread, i.e.
270 species present in more than one region. If extinction rates are high, many lineages
271 are likely to disappear soon after they arise and inevitably before they have time to
272 expand their geographic range. Accordingly, rates of vicariance are estimated to be
273 relatively low in models that incorporate lineage extinction because these scenarios
274 diminish the likelihood widespread lineages arise and decrease the opportunities for
275 vicariant speciation. On the other hand, during an in-situ speciation event, the tally of
276 local diversity increases by one species, which would then lower the probability that
277 high extinction eliminates all species. For example, consider a scenario where
278 lineage X occurring at areas A and B [in-situ] speciates to produce lineage Y in area
279 A, while the parent lineage X remains present across both A and B. Even if extinction
280 removes lineage X entirely, area A remains occupied by lineage Y. Therefore,
281 models with high rates of species extinction will be associated with high rates of in-
282 situ speciation as this results in areas that are unlikely to become devoid of all
283 species. If extinction is ignored, this process would appear to represent a range
284 contraction of lineage X, which according to our estimates, takes place at a low rate.

285 Our modelling approach simplifies the macroevolutionary dynamics taking place in
286 the region. On the one hand, we assumed that diversification rates are uniform over
287 time when in reality there are global, climate-related events that might have
288 increased or decreased the rates of diversification. For instance, changes in
289 atmospheric carbon dioxide concentration during Miocene has affected the radiation
290 of many taxa at a global scale (Aduse-Poku et al., 2022; Spriggs et al., 2014; Zachos

291 et al., 2008). On the other hand, we assumed that diversification rates are uniform in
292 space when, in fact, a combination of biotic and abiotic processes could have
293 resulted in higher speciation rates in some locations than others. Similarly, lineages
294 might experience increased probabilities of extinction in one area over another,
295 although it would be truly challenging to detect such a signal from data as molecular
296 phylogenetic trees are seldom informative on clade-wide extinction rates (Nee,
297 Holmes, et al., 1994; Rabosky, 2010), and even less suitable for detecting
298 differences in extinction rates between lineages. Although we recognise the potential
299 importance of these patterns, they are not currently represented in our models,
300 which aim to reconstruct the biogeographic history of the region when assuming
301 different extinction rates, but do not estimate extinction rates from phylogenetic trees

302 Integrating extinction dynamics into ancestral reconstructions is crucial for
303 reconciling evolutionary processes shaping the modern patterns of species diversity
304 with geological and palaeontological evidence. A similar re-evaluation of lineage
305 evolution incorporating non-zero rates of extinction was required to reconcile the
306 contemporary biogeography of hummingbirds with the fossil record and
307 demonstrated that the common ancestor of hummingbird species lived in North
308 America (Herrera-Alsina et al., 2022) rather than South America (McGuire et al.,
309 2014; McGuire et al., 2007). Our results encourage the use of interdisciplinary and
310 complementary approaches to address questions that cannot, otherwise, be
311 addressed comprehensively.

312

313

314 **Methods**

315 We collated published papers that reconstructed the biogeographic history of clades
316 in Indo-Australian Archipelago (IAA) and selected those whose geographic range
317 had limited departure from the following geographic localities: Borneo, Sulawesi,
318 Sumatra, Java, Philippines, New Guinea and continental SE Asia. The taxonomic
319 scope of these studies included plants, and both invertebrate and vertebrate
320 animals: breadfruit (*Artocarpus*; Williams et al., 2017), orchids (*Paphiopedilum*; Tsai
321 et al., 2020), treelets (*Pseuduvaria*; Su & Saunders, 2009), taros (*Alocasia*;
322 Nauheimer et al., 2012), crabs (*Parathelphusa*; Klaus et al., 2013), crickets
323 (*Cardiodactylus*; Dong et al., 2018), parachuting frogs (*Rhacophorus*; O'Connell et
324 al., 2018), and herbs (*Cyrtandra*; Atkins et al., 2020). All those studies applied either
325 DEC (Dispersal-Extinction-Cladogenesis; Ree & Smith, 2008) or DIVA(Dispersal-
326 Vicariance Analysis Matzke, 2014; Ronquist, 1997) models for biogeographic
327 reconstruction. The authors kindly provided phylogenetic trees and geographic
328 information used for their analyses.

329 We used the modelling framework LEMAD (Lineage Extinction Model of Ancestral
330 Distribution) to revisit the geographic distribution of the ancestors in these groups.
331 Unlike previous methods, LEMAD explicitly models the distribution of extinct lineages
332 in geographic reconstruction (Herrera-Alsina et al., 2022). DEC and similar
333 approaches use the set of extant species to reconstruct past changes in geographic
334 distributions, while LEMAD includes extant species but also models extinct species
335 (see below) to reconstruct the biogeographic history. The amount of historical
336 extinction in IAA is unknown but is likely to be high (Louys et al., 2007) and models
337 other than LEMAD neglect this key process. Notice that DEC and other approaches

338 consider *local* extinction (also known as extirpation) which is the change from
339 presence to absence of a lineage at a given location: a species/lineage could still
340 exist in other locations and remain extant to the present. Radically different
341 biogeographical reconstructions of regional biotas can be inferred when extinct
342 lineages and their distributions are modelled explicitly (Herrera-Alsina et al., 2022).
343 The inference of lineage extinction (hereafter extinction) rates from molecular
344 phylogenetic trees is challenging and might lead to the estimation of biased rates
345 because of taxonomic sampling issues (Nee et al. 1994) and heterogeneity of rates
346 across lineages (Rabosky 2010). LEMAD does not attempt to estimate extinction
347 rates, instead, it is used to explore the reconstructed ancestral distributions when
348 assuming different extinction rate values in order to address this important source of
349 uncertainty.

350 LEMAD generalizes the likelihood described in GeoSSE (Goldberg et al., 2011) for
351 any number of areas and is flexible to include different scenarios of geographic
352 speciation that facilitate the estimation of ancestral distribution. Like GeoSSE, the
353 change in geographic distribution of species is a result of species colonizing
354 locations (dispersal) and becoming extirpated from locations (i.e., the disappearance
355 from a local area, also known as range contraction or local extinction). Unlike
356 GeoSSE, LEMAD assumes that rates of speciation and extinction are uniform across
357 regions. Extinction is modelled as an instantaneous process across the entire range
358 of a lineage, which allows us to account for those events where populations
359 experience a sudden decline in size and are unlinked to geographic range
360 contractions (Goldberg et al., 2011). In LEMAD, both the phylogenetic tree and
361 geographic information are jointly used to carry out the calculation. A system of
362 equations is defined to represent 1) the probabilities of a given branch (i.e., an
363 existing branch) being present at the different geographic location, and 2) the
364 probabilities of a branch that, having existed at a different geographic location, went
365 extinct. For instance, consider that lineage Z can have any of three distributions
366 (area A, area B or being present in both A and B), LEMAD defines the probability of
367 lineage Z being present in A coupled with an equation that reflects the possibility of
368 an extinct lineage which was present in A before going extinct. The same
369 computation is carried out for area B and the area represented by both A and B. The
370 assumed extinction rate is defined by the user. The equations also include a term
371 that accounts for changes in geographic distributions i.e., lineages colonizing or
372 disappearing from locations. These equations are numerically integrated along all
373 the tree branches from the tree tips (using the geographic information of extant
374 lineages) to the root. Once the likelihood is optimized, these probabilities are
375 retrieved at each node along with the rate estimates for dispersal/extirpation, in-situ
376 and vicariant speciation (geographically mediated divergence resulting in allopatry,
377 i.e., complementary ranges).

378 Vicariant and in-situ speciation can be modelled in two different ways. On the one
379 hand, the DEC model (Ree & Smith, 2008) assumes that during vicariance, one of
380 the daughter lineages will be present in only one region (e.g., the four species ABC
381 and D are partitioned geographically into A-BCD or B-ACD; narrow vicariance); for
382 in-situ speciation, the DEC model allows that a population from a widespread
383 species diverges to form a new species which co-occurs with the parental one (i.e.,
384 in-situ subset). On the other hand, the DIVA model (Ronquist, 1997) assumes that
385 widespread species can split their ranges with no restriction in the number of areas
386 inhabited by daughter lineages, as long as they form complementary distributions

387 (e.g., a species present in regions A, B, C and D can split into AB-CD or A-BCD;
388 widespread vicariance). In DIVA, the in-situ subset mode is not assumed. In the
389 LEMAD framework, DEC and DIVA are different versions of the same model
390 (LEMAD_{DIVA} and LEMAD_{DEC}); they differ in the arrangement of parameters, thus their
391 likelihoods are comparable. We fit LEMAD_{DIVA} and LEMAD_{DEC} to the revisited
392 datasets. Because the current distribution of most species across revisited studies is
393 restricted to one or two areas and to be in line with the original analyses, the
394 maximum number of areas where ancestors could have inhabited was set to three.
395 In the LEMAD analysis and in contrast to some of the original IAA studies, our
396 models did not include a time-stratified component or jump dispersal.

397 For each dataset, we ran four models that differed in the assumed rates of extinction.
398 The decision on what extinction rate to assume is not straightforward. In the field of
399 macroevolution, estimates for extinction rates calculated from phylogenetic trees are
400 generally small, often close to zero, which contradicts the fossil record (Nee, May, et
401 al., 1994). We fitted a standard birth-death model (BD) to each phylogenetic tree and
402 confirmed that the extinction rate was estimated to be close to zero. With highly
403 incomplete fossil record and with no external evidence that could suggest a reliable
404 rate of extinction for the revised datasets, we took an alternative approach. Instead
405 of using those clearly underestimated extinction rates from a BD model, we assumed
406 that extinction could have been almost as frequent as speciation, as shown in
407 datasets with the most complete fossil records (Barnosky et al., 2011; Budd & Mann,
408 2018). We therefore used the speciation rate estimate under a BD for each dataset
409 and termed this rate BD_{mu}. This was the assumed extinction rate for the first
410 model. In the second model, we assumed a much higher rate of extinction (10 x
411 BD_{mu}; De Vos et al., 2015). The third model assumed low extinction (BD_{mu}/10).
412 It is reasonable to assume that the extinction rate adopted for the second and third
413 models bracket the actual range of values for each lineage, while that adopted in the
414 first model is a tentative estimate of its long-term mean. Finally, we fit models
415 assuming zero extinction. Note that during LEMAD likelihood optimization, speciation
416 and range evolution rates are adjusted according to the assumed extinction rate (i.e.,
417 speciation rate is in all cases higher than extinction). We allowed the rates of in-situ
418 and vicariant speciation and range evolution (i.e., colonization, and local extinction -
419 hereafter extirpation-) to be free parameters in the model. We found that LEMAD_{DEC}
420 models had better likelihood than LEMAD_{DIVA}, so we report the results of the former.
421 All analyses were carried out using one phylogenetic tree per clade that was
422 provided by the authors of the original papers.

423

424

425 Figure Captions

426

427 Figure 1. Geographic origins of eight clades in the Indo-Australian Archipelago. For
428 each dataset, we reconstruct the geographic distribution of the clade's common
429 ancestor while assuming intermediate and zero rates of lineage extinction.

430

431

432 Figure 2. Reconstructed species richness over time across the Indo-Australian
433 Archipelago under intermediate rates of extinction scenario for eight taxonomic
434 groups. 1: Crabs, 2: Parachuting frogs, 3: *Pseuduvaria* treelets, 4: Orchids, 5:
435 Breadfruit, 6: Taros, 7: *Cyrtandra* herbs, 8: Crickets. Colour code shows the relative
436 number of species inhabiting each location at each time point. Notice that
437 widespread ancestors contribute to the species richness of several locations. Time
438 scale on the left is in million years. Similar figures but assuming low and high rates of
439 extinction can be found in Supplementary Material.

440

441

442 Figure 3. Rates of range evolution (colonization and extirpation), in-situ and vicariant
443 speciation estimated during the reconstruction of ancestral geographic distribution
444 for eight clades. For each dataset, we modelled three different scenarios that
445 assume low, intermediate and high rates of lineage extinction.

446

447

448

449

450

451

452 **References**

- 453 Aduse-Poku, K., van Bergen, E., Sáfián, S., Collins, S. C., Etienne, R. S., Herrera-
454 Alsina, L., Brakefield, P. M., Brattström, O., Lohman, D. J., & Wahlberg, N.
455 (2022). Miocene Climate and Habitat Change Drove Diversification in *Bicyclus*,
456 Africa's Largest Radiation of Satyrine Butterflies. *Systematic Biology*, *71*(3),
457 570–588. <https://doi.org/10.1093/sysbio/syab066>
- 458 Atkins, H. J., Bramley, G. L. C., Johnson, M. A., Kartonegoro, A., Nishii, K.,
459 Kokubugata, G., Möller, M., & Hughes, M. (2020). A molecular phylogeny of
460 Southeast Asian *Cyrtandra* (Gesneriaceae) supports an emerging paradigm for
461 Malesian plant biogeography. *Frontiers of Biogeography*, *12*(1).
462 <https://doi.org/10.21425/F5FBG44184>
- 463 Barnosky, A. D., Matzke, N., Tomiya, S., Wogan, G. O. U., Swartz, B., Quental, T.
464 B., Marshall, C., McGuire, J. L., Lindsey, E. L., Maguire, K. C., Mersey, B., &
465 Ferrer, E. A. (2011). Has the Earth's sixth mass extinction already arrived? In
466 *Nature* (Vol. 471, Issue 7336, pp. 51–57). <https://doi.org/10.1038/nature09678>
- 467 Bocek, M., & Bocak, L. (2019). The origins and dispersal history of the trichaline net-
468 winged beetles in Southeast Asia, Wallacea, New Guinea and Australia.
469 *Zoological Journal of the Linnean Society*, *185*, 1079–1094.
470 <https://academic.oup.com/zoolinnean/article/185/4/1079/5298314>
- 471 Budd, G. E., & Mann, R. P. (2018). History is written by the victors: The effect of the
472 push of the past on the fossil record. *Evolution*, *72*(11), 2276–2291.
473 <https://doi.org/10.1111/evo.13593>
- 474 Carter, A., Roques, D., Bristow, C., & Kinny, P. (2001). Understanding Mesozoic
475 accretion in Southeast Asia: Significance of Triassic thermotectonism
476 (Indosinian orogeny) in Vietnam. In *Geology*. www.copyright.com
- 477 De Bruyn, M., Stelbrink, B., Morley, R. J., Hall, R., Carvalho, G. R., Cannon, C. H.,
478 Van Den Bergh, G., Meijaard, E., Metcalfe, I., Boitani, L., Maiorano, L., Shoup,
479 R., & Von Rintelen, T. (2014). Borneo and Indochina are major evolutionary
480 hotspots for Southeast Asian biodiversity. *Systematic Biology*, *63*(6), 879–901.
481 <https://doi.org/10.1093/sysbio/syu047>
- 482 Dong, J., Kergoat, G. J., Vicente, N., Rahmadi, C., Xu, S., & Robillard, T. (2018).
483 Biogeographic patterns and diversification dynamics of the genus
484 *Cardiodactylus* Saussure (Orthoptera, Grylloidea, Eneopterinae) in Southeast
485 Asia. *Molecular Phylogenetics and Evolution*, *129*, 1–14.
486 <https://doi.org/10.1016/j.ympev.2018.06.001>
- 487 Ellison, A. M., Farnsworth, E. J., & Merkt, R. E. (1999). Origins of Mangrove
488 Ecosystems and the Mangrove Biodiversity Anomaly. *Global Ecology and*
489 *Biogeography*, *8*(2), 95–115.
490 <https://www.jstor.org/stable/2997852?seq=1&cid=pdf->

- 491 Goldberg, E. E., Lancaster, L. T., & Ree, R. H. (2011). Phylogenetic inference of
492 reciprocal effects between geographic range evolution and diversification.
493 *Systematic Biology*, 60(4), 451–465. <https://doi.org/10.1093/sysbio/syr046>
- 494 Grismer, L. L., Wood Jr, P. L., Aowphol, A., Cota, M., Grismer, M. S., Murdoch, M.
495 L., Aguilar, C., & Grismer, J. L. (2016). Out of Borneo, again and again:
496 biogeography of the Stream Toad genus *Ansonia* Stoliczka (Anura: Bufonidae)
497 and the discovery of the first limestone cave-dwelling species. *Biological Journal*
498 *of the Linnean Society*, 120, 371–395.
499 <http://zoobank.org/urn:lsid:zoobank.org:pub:20A5589C-7E6F->
- 500 Grudinski, M., Wanntorp, L., Pannell, C. M., & Muellner-Riehl, A. N. (2014). West to
501 east dispersal in a widespread animal-dispersed woody angiosperm genus
502 (*Aglaia*, Meliaceae) across the Indo-Australian Archipelago. *Journal of*
503 *Biogeography*, 41(6), 1149–1159. <https://doi.org/10.1111/jbi.12280>
- 504 Hall, R. (2013). The palaeogeography of Sundaland and Wallacea since the Late
505 Jurassic. *Journal of Limnology*, 72(S2), 1–17.
506 <https://doi.org/10.4081/jlimnol.2013.s2.e1>
- 507 Herrera-Alsina, L., Algar, A. C., Lancaster, L. T., Ornelas, J. F., Bocedi, G.,
508 Papadopulos, A. S. T., Gubry-Rangin, C., Osborne, O. G., Mynard, P., Sudiana,
509 I. M., Lupiyaningdyah, P., Juliandi, B., & Travis, J. M. J. (2022). The Missing
510 Link in Biogeographic Reconstruction: Accounting for Lineage Extinction
511 Rewrites History. *Journal of Biogeography*, 49, 1941–1951.
- 512 Husson, L., Boucher, F. C., Sarr, A. C., Sepulchre, P., & Cahyarini, S. Y. (2020).
513 Evidence of Sundaland's subsidence requires revisiting its biogeography. In
514 *Journal of Biogeography* (Vol. 47, Issue 4, pp. 843–853). Blackwell Publishing
515 Ltd. <https://doi.org/10.1111/jbi.13762>
- 516 Klaus, S., Selvandran, S., Goh, J. W., Wowor, D., Brandis, D., Koller, P., Schubart,
517 C. D., Streit, B., Meier, R., Ng, P. K. L., & Yeo, D. C. J. (2013). Out of Borneo:
518 Neogene diversification of Sundaic freshwater crabs (Crustacea: Brachyura:
519 Gecarcinucidae: Parathelphusa). *Journal of Biogeography*, 40(1), 63–74.
520 <https://doi.org/10.1111/j.1365-2699.2012.02771.x>
- 521 Lian, L., Peng, H. W., Erst, A. S., Ortiz, R. del C., Jabbour, F., Chen, Z. D., & Wang,
522 W. (2024). Bayesian tip-dated phylogeny and biogeography of Cissampelideae
523 (Menispermaceae): Mitigating the effects of homoplastic morphological
524 characters. *Cladistics*. <https://doi.org/10.1111/cla.12573>
- 525 Lohman, D. J., De Bruyn, M., Page, T., Von Rintelen, K., Hall, R., Ng, P. K. L., Shih,
526 H. Te, Carvalho, G. C., & Von Rintelen, T. (2011). Beyond Wallaces line: Genes
527 and biology inform historical biogeographical insights in the Indo-Australian
528 archipelago. *Annual Review of Ecology, Evolution, and Systematics*, 42.
529 <https://doi.org/10.1146/annurev-ecolsys-102710-145001>
- 530 Louys, J., Curnoe, D., & Tong, H. (2007). Characteristics of Pleistocene megafauna
531 extinctions in Southeast Asia. *Palaeogeography, Palaeoclimatology,*

- 532 *Palaeoecology*, 243(1–2), 152–173.
533 <https://doi.org/10.1016/j.palaeo.2006.07.011>
- 534 Matzke, N. J. (2014). Model selection in historical biogeography reveals that founder-
535 event speciation is a crucial process in island clades. *Systematic Biology*, 63(6),
536 951–970. <https://doi.org/10.1093/sysbio/syu056>
- 537 McGuire, J. A., Witt, C. C., Altshuler, D. L., & Remsen, J. V. (2007). Phylogenetic
538 systematics and biogeography of hummingbirds: Bayesian and maximum
539 likelihood analyses of partitioned data and selection of an appropriate
540 partitioning strategy. *Systematic Biology*, 56(5), 837–856.
541 <https://doi.org/10.1080/10635150701656360>
- 542 McGuire, J., Witt, C., Remsen, J., Corl, a, Rabosky, D., Altshuler, D., & Dudley, R.
543 (2014). Molecular phylogenetics and the diversification of hummingbirds.
544 *Current Biology*, 24, 910–196.
- 545 Nauheimer, L., Boyce, P. C., & Renner, S. S. (2012). Giant taro and its relatives: A
546 phylogeny of the large genus *Alocasia* (Araceae) sheds light on Miocene floristic
547 exchange in the Malesian region. *Molecular Phylogenetics and Evolution*, 63(1),
548 43–51. <https://doi.org/10.1016/j.ympev.2011.12.011>
- 549 Nee, S., Holmes, E. C., May, R. M., Harvey, P. H., Harvey, P. H., Nee, S., Holmes,
550 E. C., & May, R. M. (1994). Extinction rates can be estimated from molecular
551 phylogenies. *Philosophical Transactions: Biological Sciences*, 344(1307), 77–
552 82.
- 553 Nee, S., May, R. M., & Harvey, P. H. (1994). The reconstructed evolutionary
554 process. *Philosophical Transactions of the Royal Society B: Biological Sciences*,
555 344(1309), 305–311. <https://doi.org/10.1098/rstb.1994.0068>
- 556 O'Connell, K. A., Smart, U., Smith, E. N., Hamidy, A., Kurniawan, N., & Fujita, M. K.
557 (2018). Within-island diversification underlies parachuting frog (*Rhacophorus*)
558 species accumulation on the Sunda Shelf. *Journal of Biogeography*, 45(4), 929–
559 940. <https://doi.org/10.1111/jbi.13162>
- 560 Rabosky, D. L. (2010). Extinction rates should not be estimated from molecular
561 phylogenies. *Evolution*, 64(6), 1816–1824. <https://doi.org/10.1111/j.1558-5646.2009.00926.x>
- 563 Ree, R. H., & Smith, S. A. (2008). Maximum likelihood inference of geographic range
564 evolution by dispersal, local extinction, and cladogenesis. *Systematic Biology*,
565 57(1), 4–14. <https://doi.org/10.1080/10635150701883881>
- 566 Renema, W., Bellwood, D. R., Braga, J. C., Bromfield, K., Hall, R., Johnson, K. G.,
567 Lunt, P., Meyer, C. P., Mcmonagle, L. B., Morley, R. J., O'dea, A., Todd, J. A.,
568 Wesselingh, F. P., Wilson, M. E. J., & Pandolfi, J. M. (2008). Hopping Hotspots:
569 Global Shifts in Marine Biodiversity. *Science*, 321, 654–657.
570 <https://www.science.org>

- 571 Ronquist, F. (1997). Dispersal-Vicariance Analysis: A New Approach to the
572 Quantification of Historical Biogeography. *Systematic Biology*, 46(1), 195–203.
573 <https://doi.org/10.1093/sysbio/46.1.195>
- 574 Salles, T., Mallard, C., Husson, L., Zahirovic, S., Sarr, A. C., & Sepulchre, P. (2021).
575 Quaternary landscape dynamics boosted species dispersal across Southeast
576 Asia. *Communications Earth and Environment*, 2(1).
577 <https://doi.org/10.1038/s43247-021-00311-7>
- 578 Sarr, A. C., Husson, L., Sepulchre, P., Pastier, A. M., Pedoja, K., Elliot, M., Arias-
579 Ruiz, C., Solihuddin, T., Aribowo, S., & Susilohadi. (2019). Subsiding sundaland.
580 *Geology*, 47(2), 119–122. <https://doi.org/10.1130/G45629.1>
- 581 Simaiakis, S. M., Dimopoulou, A., Mitrakos, A., Mylonas, M., & Parmakelis, A.
582 (2012). The evolutionary history of the Mediterranean centipede *Scolopendra*
583 *cingulata* (Latreille, 1829) (Chilopoda: Scolopendridae) across the Aegean
584 archipelago. *Biological Journal of the Linnean Society*, 105, 507–521.
585 <https://academic.oup.com/biolinnean/article/105/3/507/2452642>
- 586 Spriggs, E. L., Christinb, P. A., & Edwards, E. J. (2014). C4 photosynthesis
587 promoted species diversification during the miocene grassland expansion. *PLoS*
588 *ONE*, 9(5). <https://doi.org/10.1371/journal.pone.0097722>
- 589 Su, Y. C. F., & Saunders, R. M. K. (2009). Evolutionary divergence times in the
590 Annonaceae: Evidence of a late Miocene origin of *Pseuduvaria* in Sundaland
591 with subsequent diversification in New Guinea. *BMC Evolutionary Biology*, 9(1).
592 <https://doi.org/10.1186/1471-2148-9-153>
- 593 Sýkora, V., Herrera-Alsina, L., Maier, C., Martínez-Román, N. R., Archangelsky, M.,
594 Bilton, D. T., Seidel, M., Leschen, R. A. B., & Fikáček, M. (2023). Reconstructing
595 ancient dispersal through Antarctica: A case study of stream-inhabiting beetles.
596 *Journal of Biogeography*, 50(11), 1939–1954. <https://doi.org/10.1111/jbi.14702>
- 597 Thomas, D. C., Hughes, M., Phutthai, T., Ardi, W. H., Rajbhandary, S., Rubite, R.,
598 Twyford, A. D., & Richardson, J. E. (2012). West to east dispersal and
599 subsequent rapid diversification of the mega-diverse genus *Begonia*
600 (*Begoniaceae*) in the Malesian archipelago. *Journal of Biogeography*, 39(1), 98–
601 113. <https://doi.org/10.1111/j.1365-2699.2011.02596.x>
- 602 Tsai, C. C., Liao, P. C., Ko, Y. Z., Chen, C. H., & Chiang, Y. C. (2020). Phylogeny
603 and Historical Biogeography of *Paphiopedilum* Pfitzer (*Orchidaceae*) Based on
604 Nuclear and Plastid DNA. *Frontiers in Plant Science*, 11.
605 <https://doi.org/10.3389/fpls.2020.00126>
- 606 Williams, E. W., Gardner, E. M., Harris, R., Chaveerach, A., Pereira, J. T., & Zerega,
607 N. J. C. (2017). Out of Borneo: Biogeography, phylogeny and divergence date
608 estimates of *Artocarpus* (*Moraceae*). *Annals of Botany*, 119(4), 611–627.
609 <https://doi.org/10.1093/aob/mcw249>
- 610 Yasuhara, M., Iwatani, H., Hunt, G., Okahashi, H., Kase, T., Hayashi, H., Irizuki, T.,
611 Aguilar, Y. M., Fernando, A. G. S., & Renema, W. (2017). Cenozoic dynamics of

612 shallow-marine biodiversity in the Western Pacific. *Journal of Biogeography*,
613 44(3), 567–578. <https://doi.org/10.1111/jbi.12880>

















614 Zachos, J. C., Dickens, G. R., & Zeebe, R. E. (2008). An early Cenozoic perspective
615 on greenhouse warming and carbon-cycle dynamics. In *Nature* (Vol. 451, Issue
616 7176, pp. 279–283). Nature Publishing Group.
617 <https://doi.org/10.1038/nature06588>

618 Zahirovic, S., Seton, M., & Müller, R. D. (2014). The Cretaceous and Cenozoic
619 tectonic evolution of Southeast Asia. *Solid Earth*, 5(1), 227–273.
620 <https://doi.org/10.5194/se-5-227-2014>

621

622

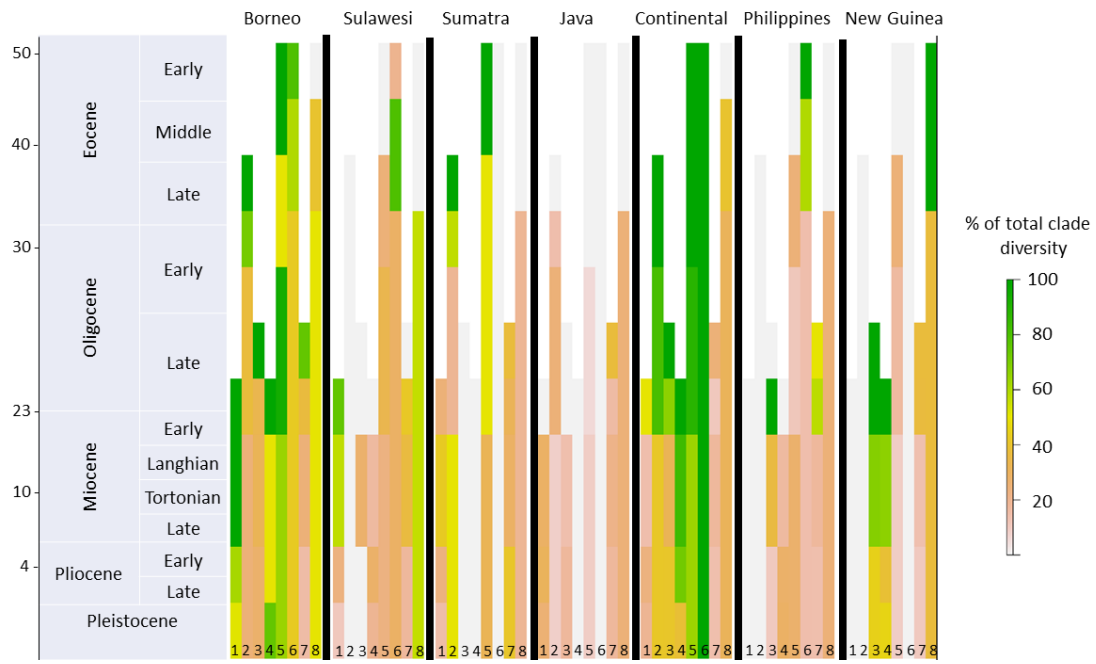
623 **Figure 1**

Group	Geographic origin when extinction modelled	Geographic origin when extinction = 0.
Breadfruit		
Orchids		
Pseuduvaria treelets		
Taros		
Crabs		
Crickets		
Parachuting frogs		
Cyrtandra herbs		

624

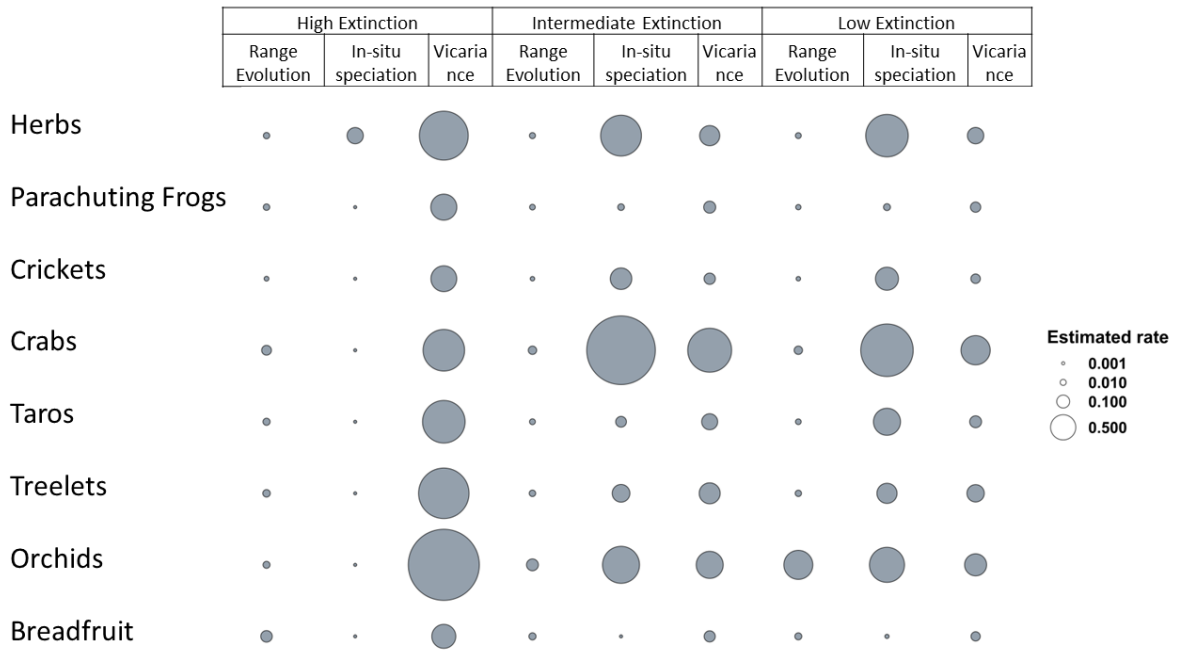
625

626 **Figure 2**



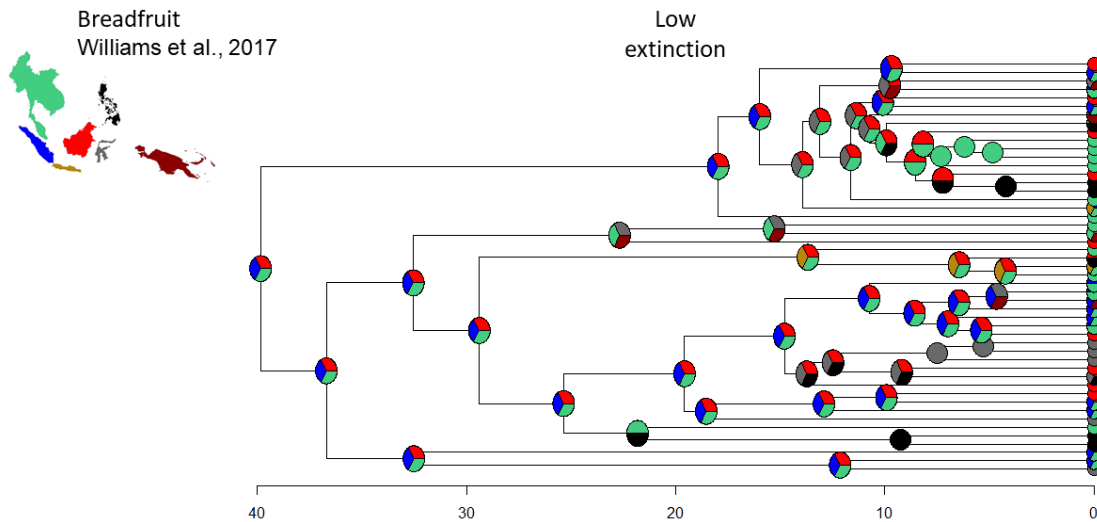
627

628

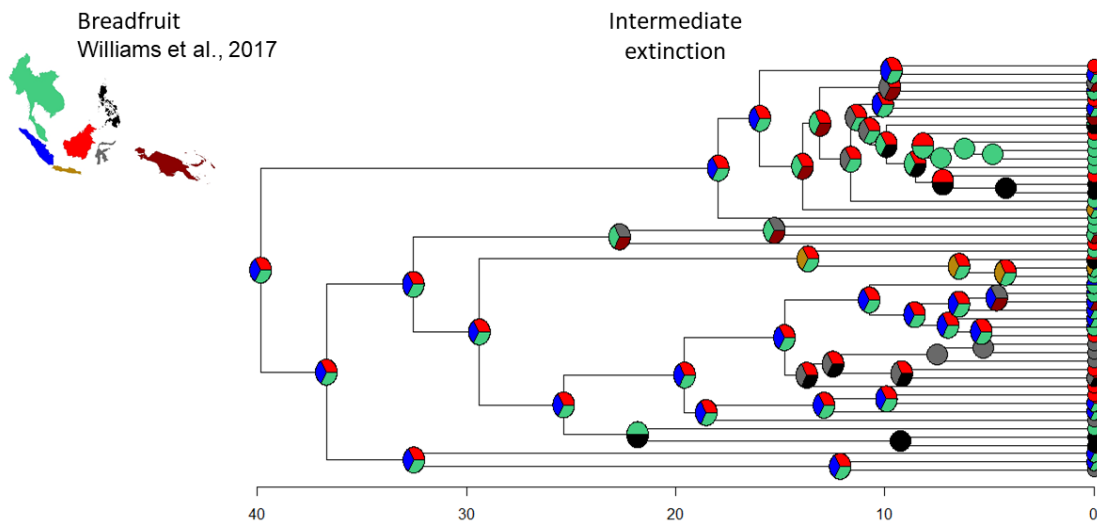


630

631

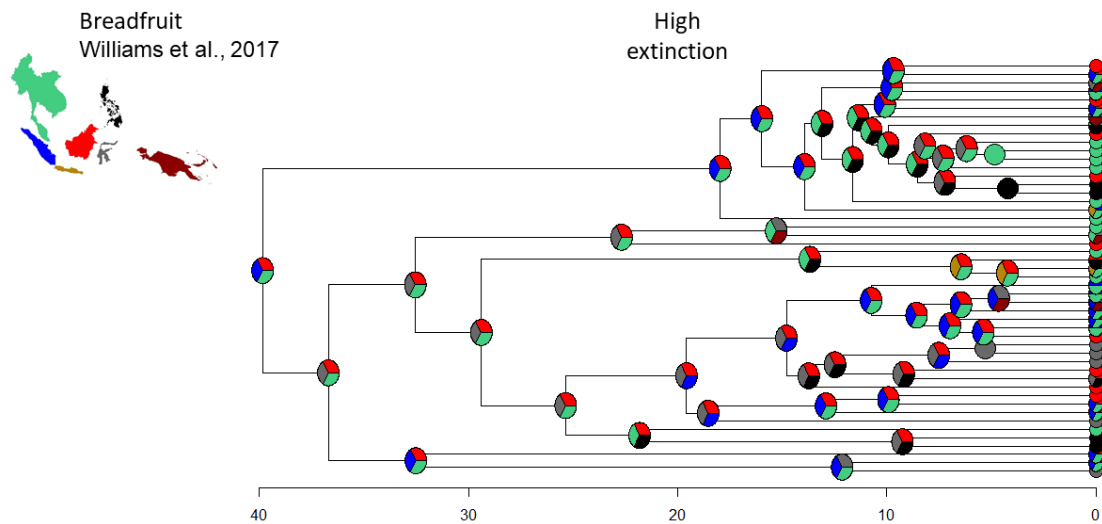


635 Figure S1. Ancestral distribution of breadfruit species (*Artocarpus*) reconstructed
636 using LEMAD (Lineage Extinction Model of Ancestral Distribution) and assuming that
637 extinction rate is one-tenth of the speciation rate estimated from fitting a birth-death
638 model to the phylogenetic tree. Nodes with more than one colour indicate that the
639 distribution for that ancestor is estimated to include more than one area. Note that
640 speciation rate will be adjusted accordingly during the likelihood optimization.



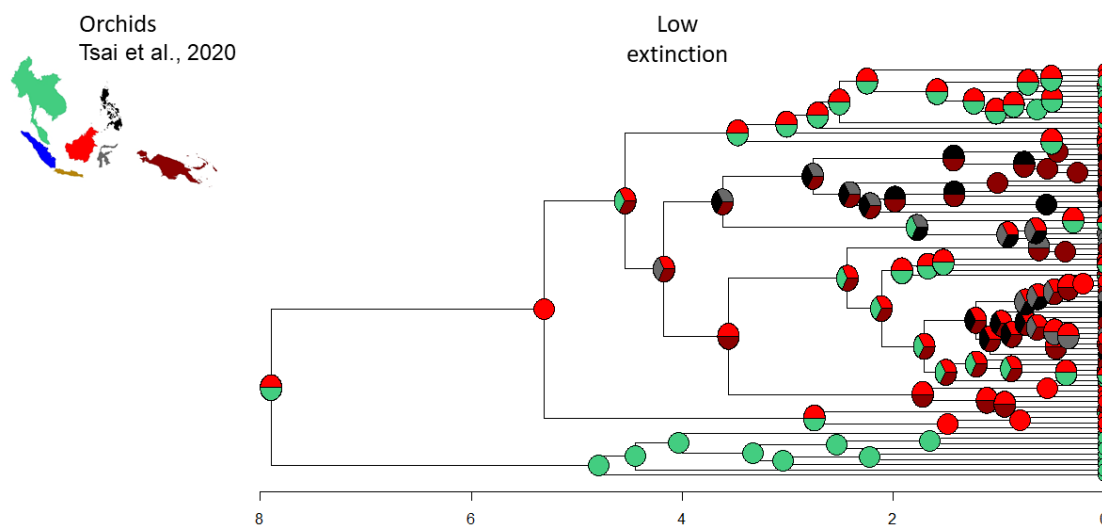
642 Figure S2. Ancestral distribution of breadfruit species (*Artocarpus*) reconstructed
643 using LEMAD (Lineage Extinction Model of Ancestral Distribution) and assuming that

644 extinction rate equals the speciation rate estimated from fitting a birth-death model to
645 the phylogenetic tree. Nodes with more than one colour indicate that the distribution
646 for that ancestor is estimated to include more than one area. Note that speciation
647 rate will be adjusted accordingly during the likelihood optimization.



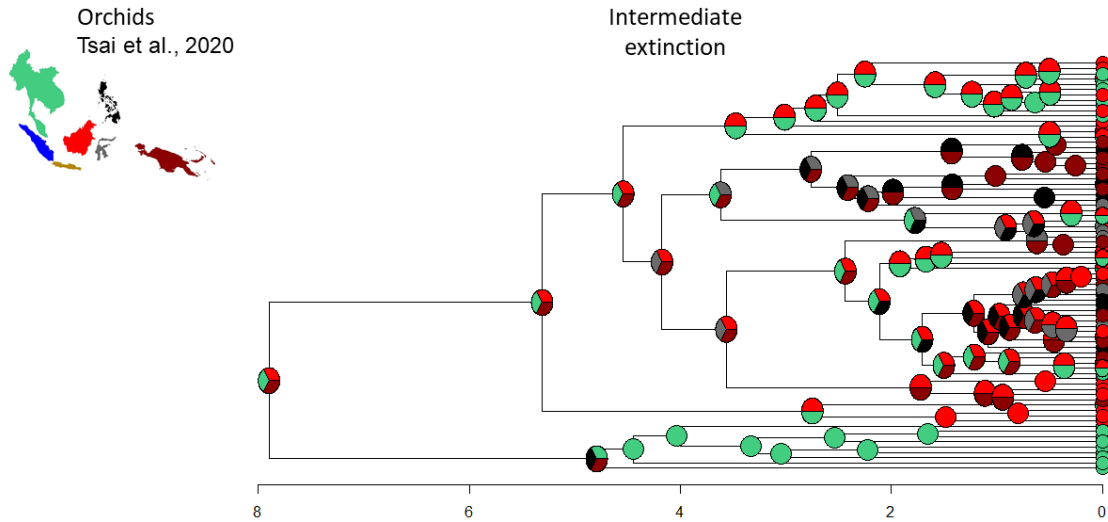
648
649 Figure S3. Ancestral distribution of breadfruit species (*Artocarpus*) reconstructed
650 using LEMAD (Lineage Extinction Model of Ancestral Distribution) and assuming that
651 extinction rate is ten times the speciation rate estimated from fitting a birth-death
652 model to the phylogenetic tree. Nodes with more than one colour indicate that the
653 distribution for that ancestor is estimated to include more than one area. Note that
654 speciation rate will be adjusted accordingly during the likelihood optimization.

655



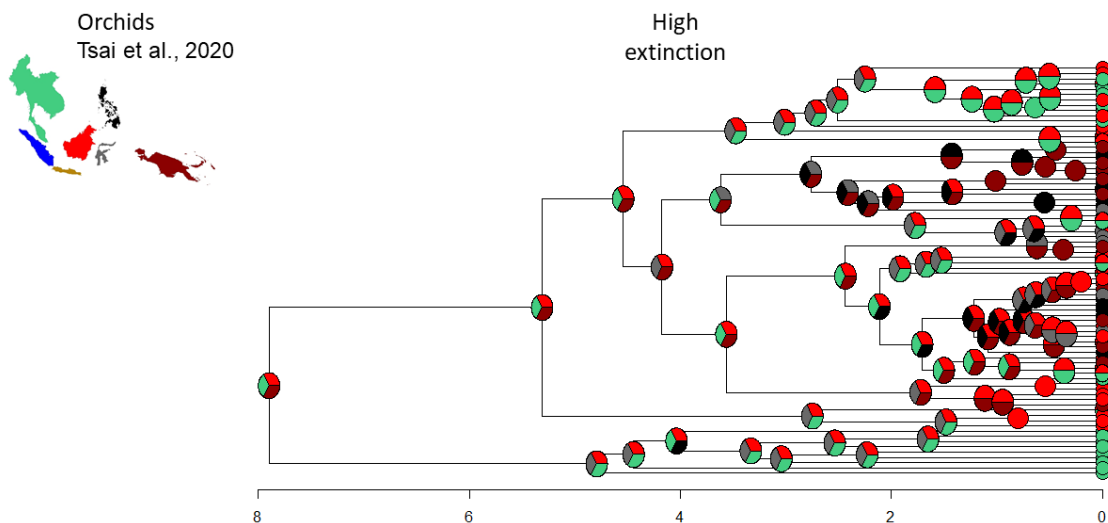
656

657 Figure S4. Ancestral distribution of orchid species (*Paphiopedilum*) reconstructed
658 using LEMAD (Lineage Extinction Model of Ancestral Distribution) and assuming that
659 extinction rate is one-tenth of the speciation rate estimated from fitting a birth-death
660 model to the phylogenetic tree. Nodes with more than one colour indicate that the
661 distribution for that ancestor is estimated to include more than one area. Note that
662 speciation rate will be adjusted accordingly during the likelihood optimization.



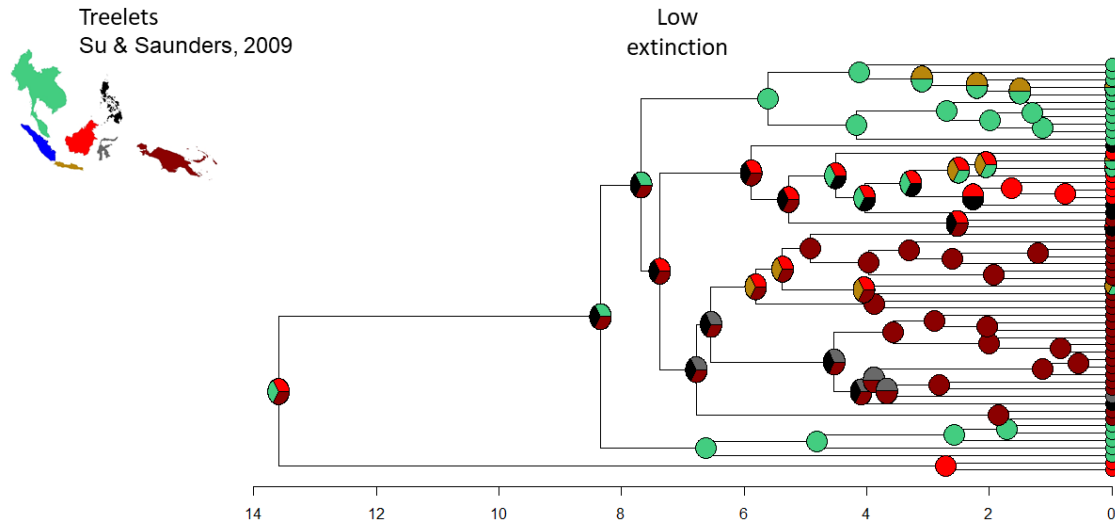
663

664 Figure S5. Ancestral distribution of orchid species (*Paphiopedilum*) reconstructed
665 using LEMAD (Lineage Extinction Model of Ancestral Distribution) and assuming that
666 extinction rate equals the speciation rate estimated from fitting a birth-death model to
667 the phylogenetic tree. Nodes with more than one colour indicate that the distribution
668 for that ancestor is estimated to include more than one area. Note that speciation
669 rate will be adjusted accordingly during the likelihood optimization.



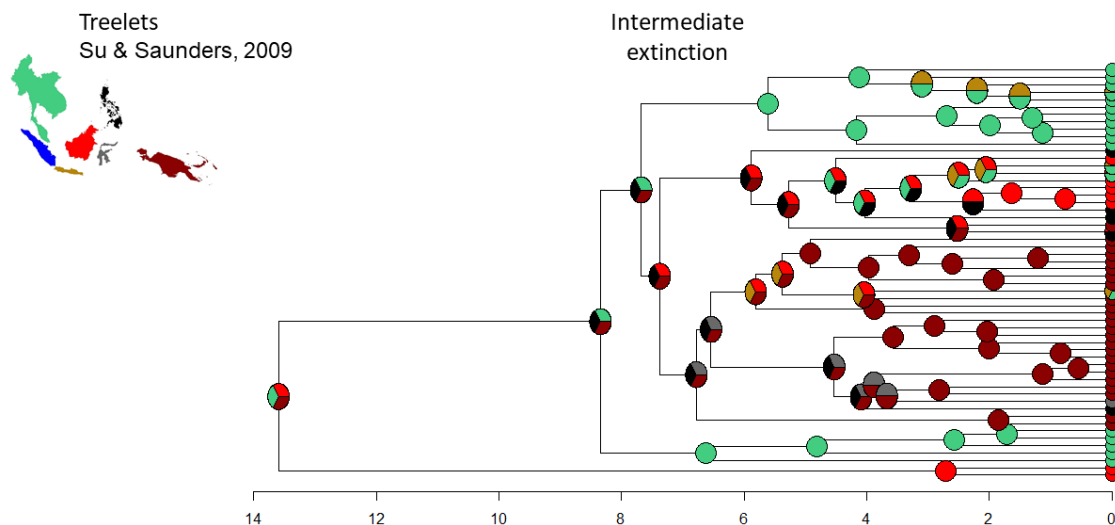
670

671 Figure S6. Ancestral distribution of orchid species (*Paphiopedilum*) reconstructed
672 using LEMAD (Lineage Extinction Model of Ancestral Distribution) and assuming that
673 extinction rate is ten times the speciation rate estimated from fitting a birth-death
674 model to the phylogenetic tree. Nodes with more than one colour indicate that the
675 distribution for that ancestor is estimated to include more than one area. Note that
676 speciation rate will be adjusted accordingly during the likelihood optimization.



677

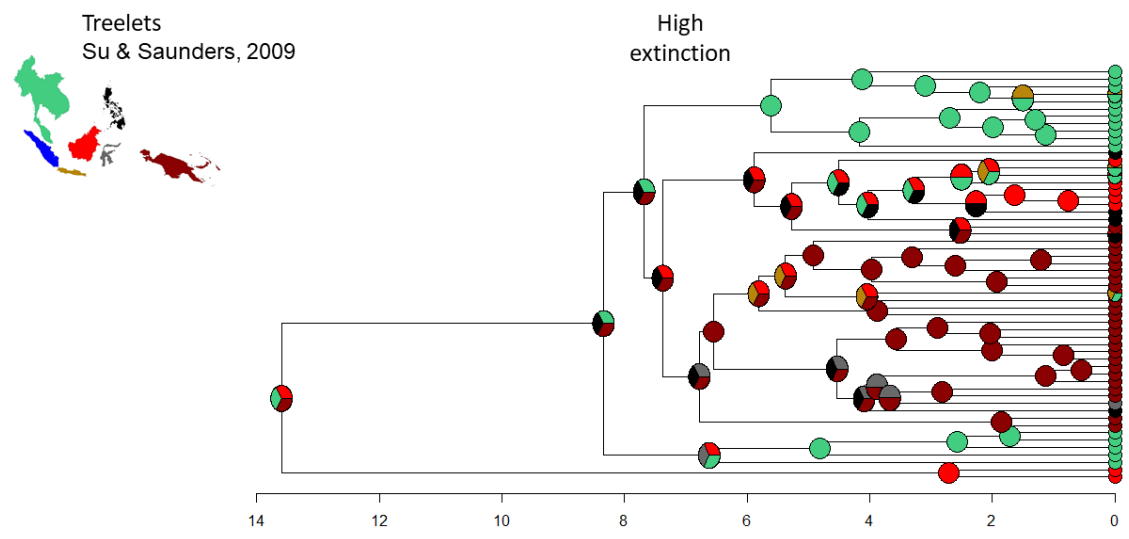
678 Figure S7. Ancestral distribution of treelet species (*Pseuduvaria*) reconstructed using
679 LEMAD (Lineage Extinction Model of Ancestral Distribution) and assuming that
680 extinction rate is one-tenth of the speciation rate estimated from fitting a birth-death
681 model to the phylogenetic tree. Nodes with more than one colour indicate that the
682 distribution for that ancestor is estimated to include more than one area. Note that
683 speciation rate will be adjusted accordingly during the likelihood optimization.



684

685 Figure S8. Ancestral distribution of treelet species (*Pseuduvaria*) reconstructed using
686 LEMAD (Lineage Extinction Model of Ancestral Distribution) and assuming that
687 extinction rate equals the speciation rate estimated from fitting a birth-death model to
688 the phylogenetic tree. Nodes with more than one colour indicate that the distribution
689 for that ancestor is estimated to include more than one area. Note that speciation
690 rate will be adjusted accordingly during the likelihood optimization.

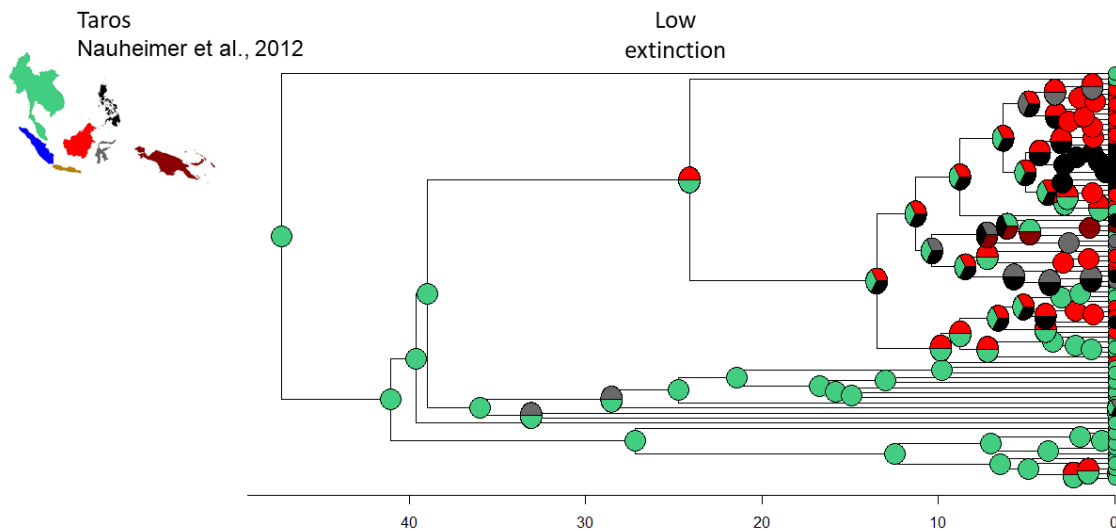
691



692

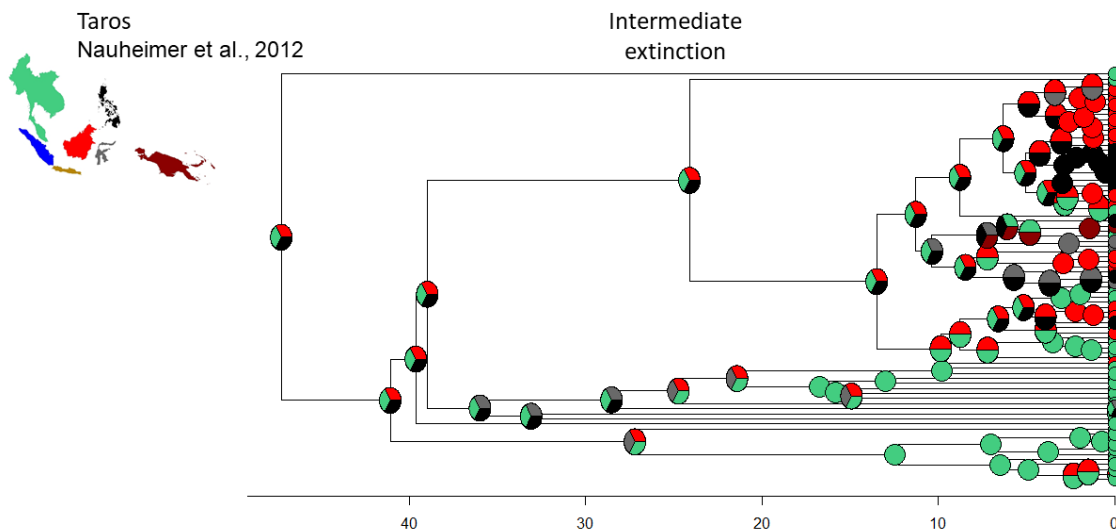
693 Figure S9. Ancestral distribution of treelet species (*Pseuduvaria*) reconstructed using
694 LEMAD (Lineage Extinction Model of Ancestral Distribution) and assuming that
695 extinction rate is ten times the speciation rate estimated from fitting a birth-death
696 model to the phylogenetic tree. Nodes with more than one colour indicate that the
697 distribution for that ancestor is estimated to include more than one area. Note that
698 speciation rate will be adjusted accordingly during the likelihood optimization.

699



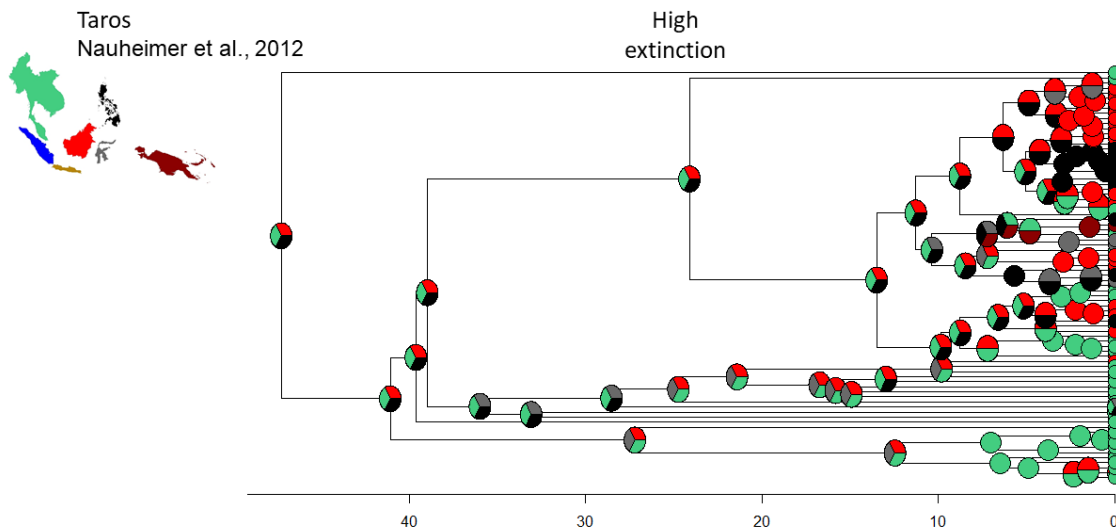
700

701 Figure S10. Ancestral distribution of taro species (*Alocasia*) reconstructed using
 702 LEMAD (Lineage Extinction Model of Ancestral Distribution) and assuming that
 703 extinction rate is one-tenth of the speciation rate estimated from fitting a birth-death
 704 model to the phylogenetic tree. Nodes with more than one colour indicate that the
 705 distribution for that ancestor is estimated to include more than one area. Note that
 706 speciation rate will be adjusted accordingly during the likelihood optimization.



707

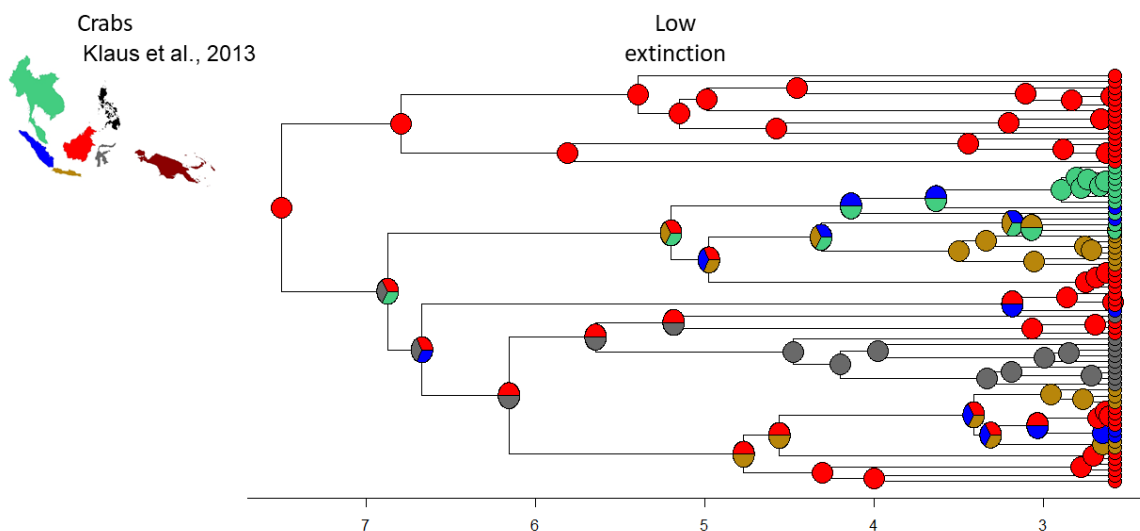
708 Figure S11. Ancestral distribution of taro species (*Alocasia*) reconstructed using
 709 LEMAD (Lineage Extinction Model of Ancestral Distribution) and assuming that
 710 extinction rate equals the speciation rate estimated from fitting a birth-death model to
 711 the phylogenetic tree. Nodes with more than one colour indicate that the distribution
 712 for that ancestor is estimated to include more than one area. Note that speciation
 713 rate will be adjusted accordingly during the likelihood optimization.



714

715 Figure S12. Ancestral distribution of taro species (*Allocaisia*) reconstructed using
 716 LEMAD (Lineage Extinction Model of Ancestral Distribution) and assuming that
 717 extinction rate is ten times the speciation rate estimated from fitting a birth-death
 718 model to the phylogenetic tree. Nodes with more than one colour indicate that the
 719 distribution for that ancestor is estimated to include more than one area. Note that
 720 speciation rate will be adjusted accordingly during the likelihood optimization.

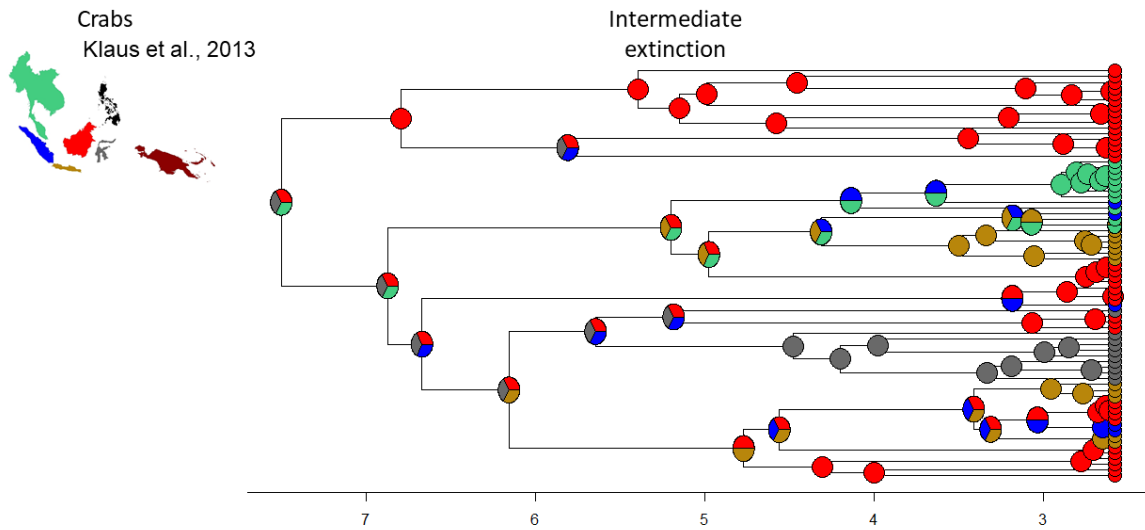
721



722

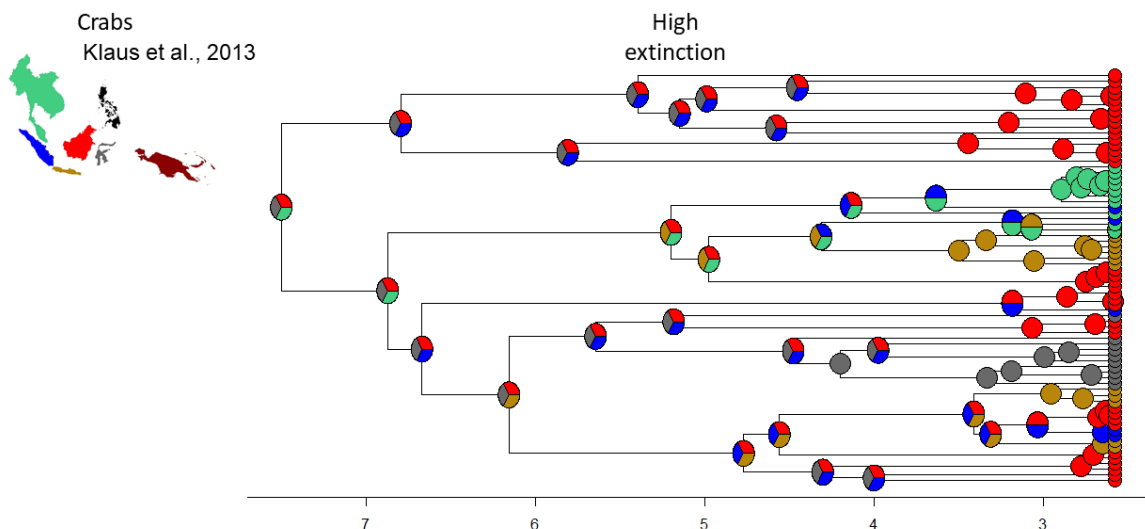
723 Figure S13. Ancestral distribution of crab species (*Parathelphusa*) reconstructed
 724 using LEMAD (Lineage Extinction Model of Ancestral Distribution) and assuming that
 725 extinction rate is one-tenth of the speciation rate estimated from fitting a birth-death
 726 model to the phylogenetic tree. Nodes with more than one colour indicate that the

727 distribution for that ancestor is estimated to include more than one area. Note that
728 speciation rate will be adjusted accordingly during the likelihood optimization.



729

730 Figure S14. Ancestral distribution of crab species (*Parathelphusa*) reconstructed
731 using LEMAD (Lineage Extinction Model of Ancestral Distribution) and assuming that
732 extinction rate equals the speciation rate estimated from fitting a birth-death model to
733 the phylogenetic tree. Nodes with more than one colour indicate that the distribution
734 for that ancestor is estimated to include more than one area. Note that speciation
735 rate will be adjusted accordingly during the likelihood optimization.

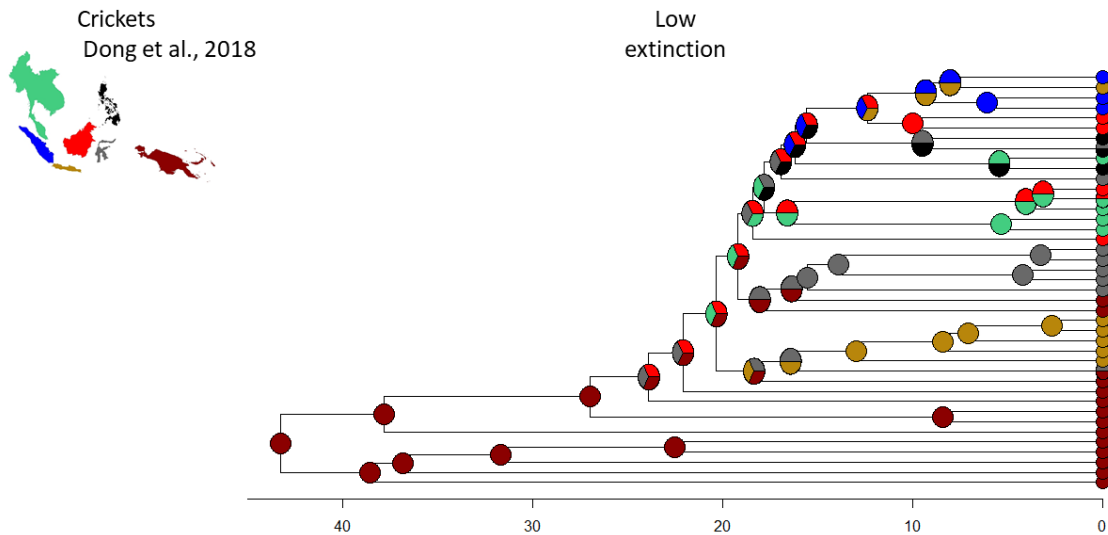


736

737 Figure S15. Ancestral distribution of crab species (*Parathelphusa*) reconstructed
738 using LEMAD (Lineage Extinction Model of Ancestral Distribution) and assuming that
739 extinction rate is ten times the speciation rate estimated from fitting a birth-death

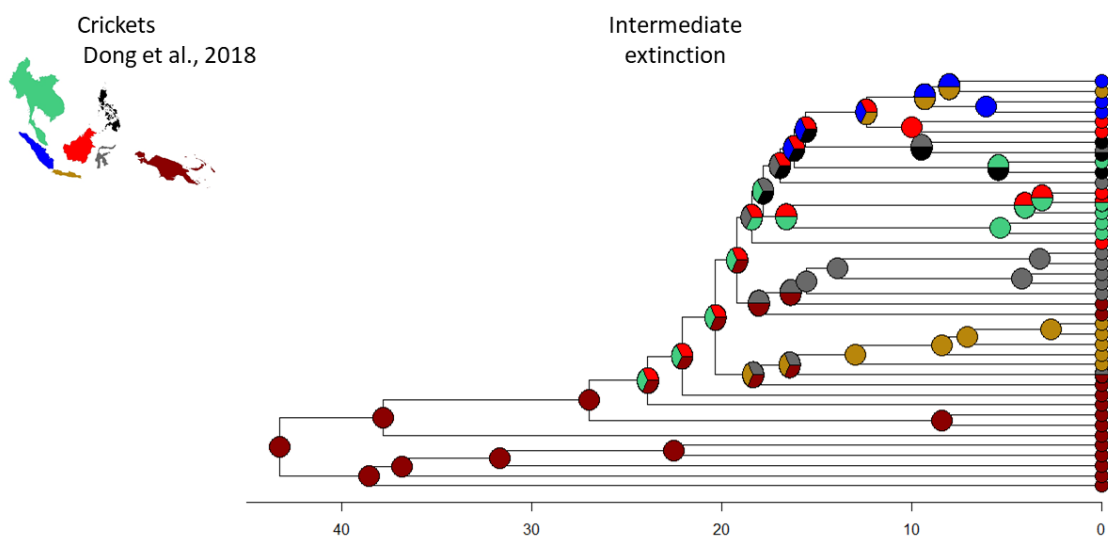
740 model to the phylogenetic tree. Nodes with more than one colour indicate that the
741 distribution for that ancestor is estimated to include more than one area. Note that
742 speciation rate will be adjusted accordingly during the likelihood optimization.

743



744

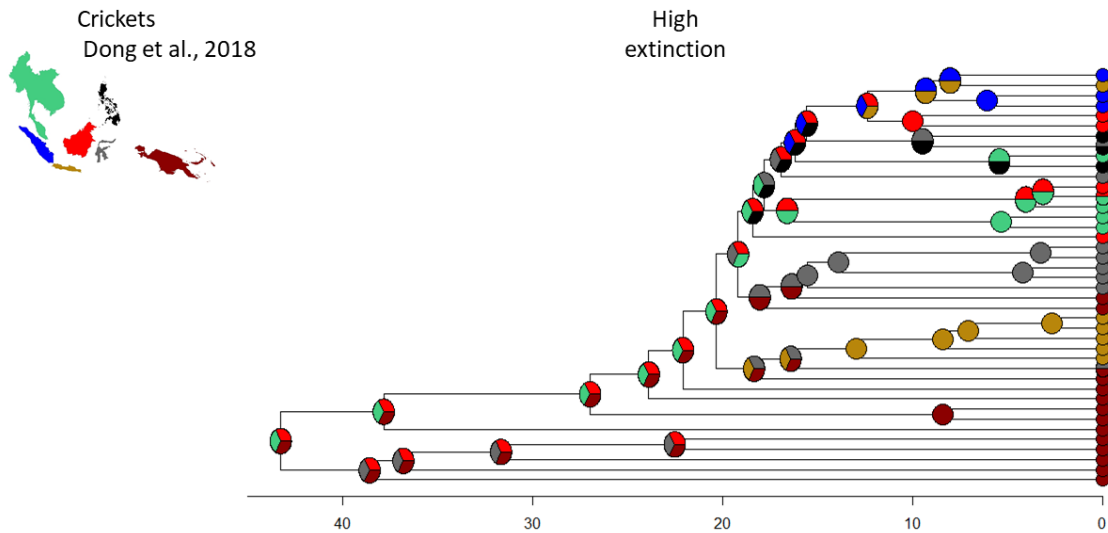
745 Figure S16. Ancestral distribution of cricket species (*Cardiodactylus*) reconstructed
746 using LEMAD (Lineage Extinction Model of Ancestral Distribution) and assuming that
747 extinction rate is one-tenth of the speciation rate estimated from fitting a birth-death
748 model to the phylogenetic tree. Nodes with more than one colour indicate that the
749 distribution for that ancestor is estimated to include more than one area. Note that
750 speciation rate will be adjusted accordingly during the likelihood optimization.



751

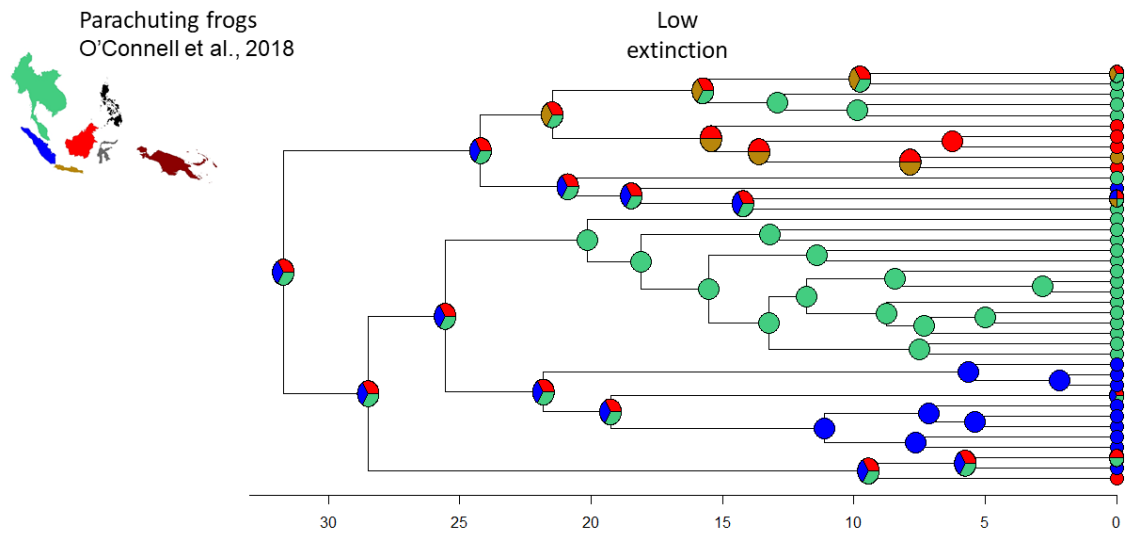
752 Figure S17. Ancestral distribution of cricket species (*Cardiodactylus*) reconstructed
753 using LEMAD (Lineage Extinction Model of Ancestral Distribution) and assuming that
754 extinction rate equals the speciation rate estimated from fitting a birth-death model to
755 the phylogenetic tree. Nodes with more than one colour indicate that the distribution
756 for that ancestor is estimated to include more than one area. Note that speciation
757 rate will be adjusted accordingly during the likelihood optimization.

758



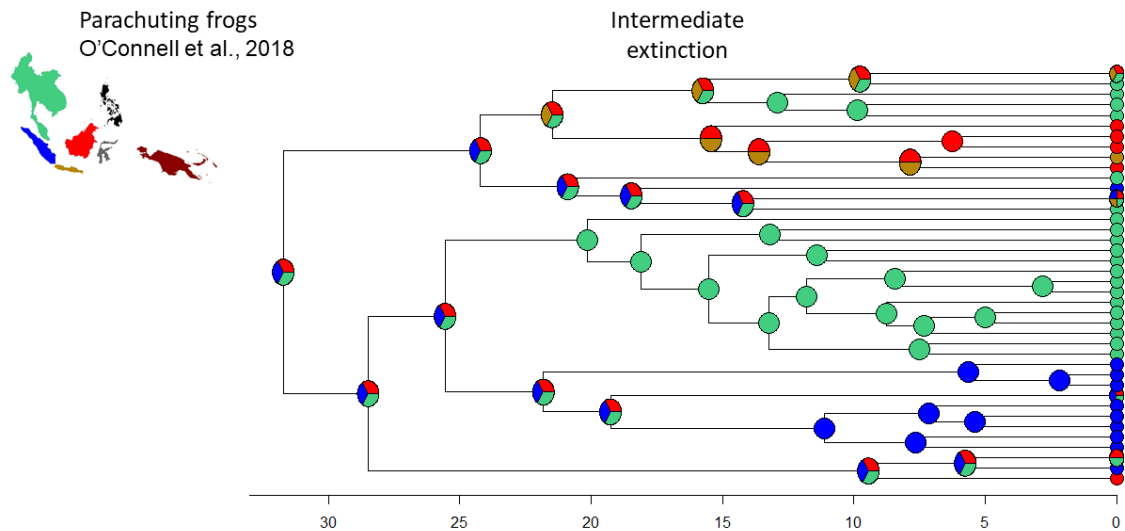
759

760 Figure S18. Ancestral distribution of cricket species (*Cardiodactylus*) reconstructed
761 using LEMAD (Lineage Extinction Model of Ancestral Distribution) and assuming that
762 extinction rate is ten times the speciation rate estimated from fitting a birth-death
763 model to the phylogenetic tree. Nodes with more than one colour indicate that the
764 distribution for that ancestor is estimated to include more than one area. Note that
765 speciation rate will be adjusted accordingly during the likelihood optimization.



766

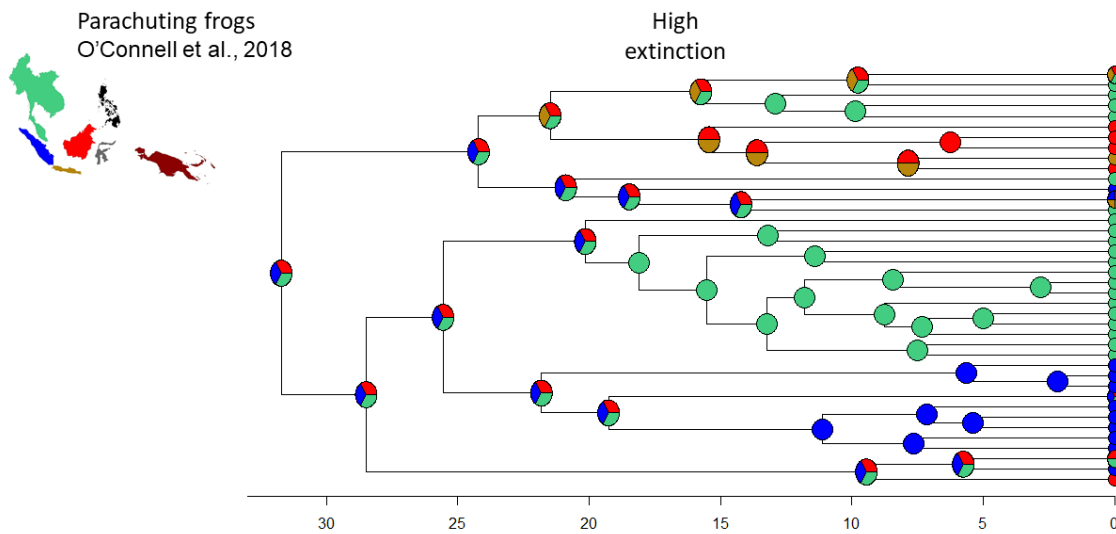
767 Figure S19. Ancestral distribution of parachuting frog species (*Rhacophorus*)
 768 reconstructed using LEMAD (Lineage Extinction Model of Ancestral Distribution) and
 769 assuming that extinction rate is one-tenth of the speciation rate estimated from fitting
 770 a birth-death model to the phylogenetic tree. Nodes with more than one colour
 771 indicate that the distribution for that ancestor is estimated to include more than one
 772 area. Note that speciation rate will be adjusted accordingly during the likelihood
 773 optimization.



774

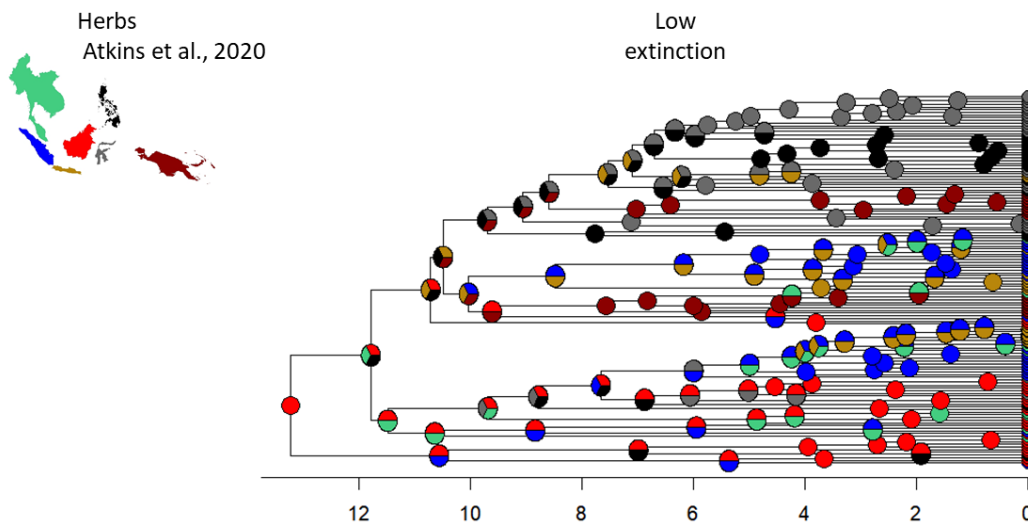
775 Figure S20. Ancestral distribution of parachuting frog species (*Rhacophorus*)
 776 reconstructed using LEMAD (Lineage Extinction Model of Ancestral Distribution) and
 777 assuming that extinction rate equals the speciation rate estimated from fitting a birth-
 778 death model to the phylogenetic tree. Nodes with more than one colour indicate that

779 the distribution for that ancestor is estimated to include more than one area. Note
780 that speciation rate will be adjusted accordingly during the likelihood optimization.



781

782 Figure S21. Ancestral distribution of parachuting frog species (*Rhacophorus*)
783 reconstructed using LEMAD (Lineage Extinction Model of Ancestral Distribution) and
784 assuming that extinction rate is ten times the speciation rate estimated from fitting a
785 birth-death model to the phylogenetic tree. Nodes with more than one colour indicate
786 that the distribution for that ancestor is estimated to include more than one area.
787 Note that speciation rate will be adjusted accordingly during the likelihood
788 optimization.

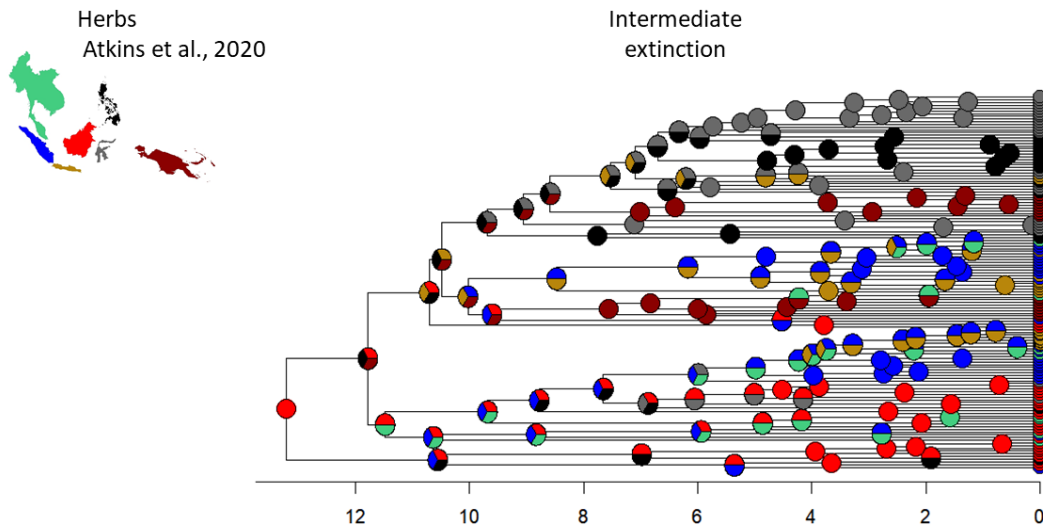


789

790

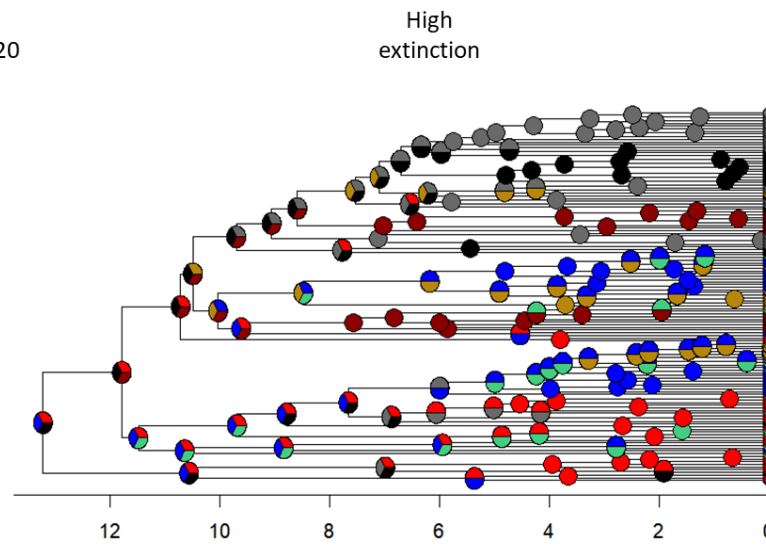
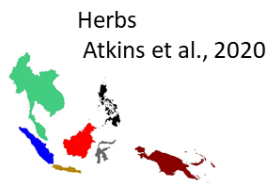
791

792 Figure S22. Ancestral distribution of tree species (*Cyrtandra*) reconstructed using
793 LEMAD (Lineage Extinction Model of Ancestral Distribution) and assuming that
794 extinction rate is one-tenth of speciation rate estimated from fitting a birth-death
795 model to the phylogenetic tree. Nodes with more than one colour indicate that the
796 distribution for that ancestor is estimated to include more than one area. Note that
797 speciation rate will be adjusted accordingly during the likelihood optimization.



798

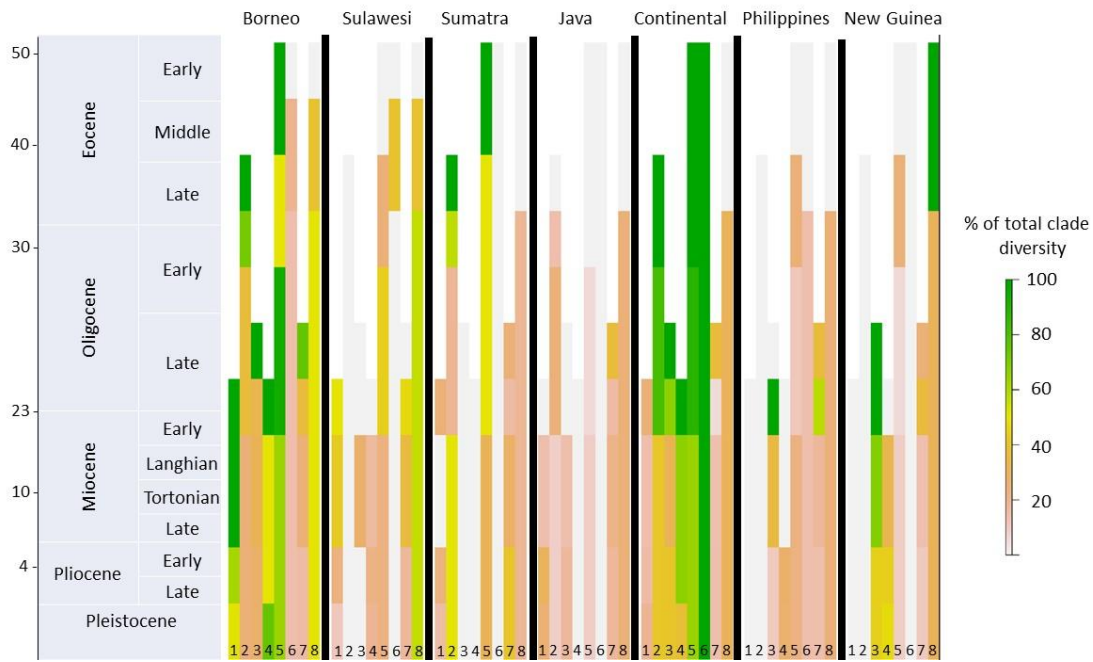
799 Figure S23. Ancestral distribution of tree species (*Cyrtandra*) reconstructed using
800 LEMAD (Lineage Extinction Model of Ancestral Distribution) and assuming that
801 extinction rate equals the speciation rate estimated from fitting a birth-death model to
802 the phylogenetic tree. Nodes with more than one colour indicate that the distribution
803 for that ancestor is estimated to include more than one area. Note that speciation
804 rate will be adjusted accordingly during the likelihood optimization



805

806 Figure S24. Ancestral distribution of tree species (*Cyrtandra*) reconstructed using
807 LEMAD (Lineage Extinction Model of Ancestral Distribution) and assuming that
808 extinction rate is ten times the speciation rate estimated from fitting a birth-death
809 model to the phylogenetic tree. Nodes with more than one colour indicate that the
810 distribution for that ancestor is estimated to include more than one area. Note that
811 speciation rate will be adjusted accordingly during the likelihood optimization.

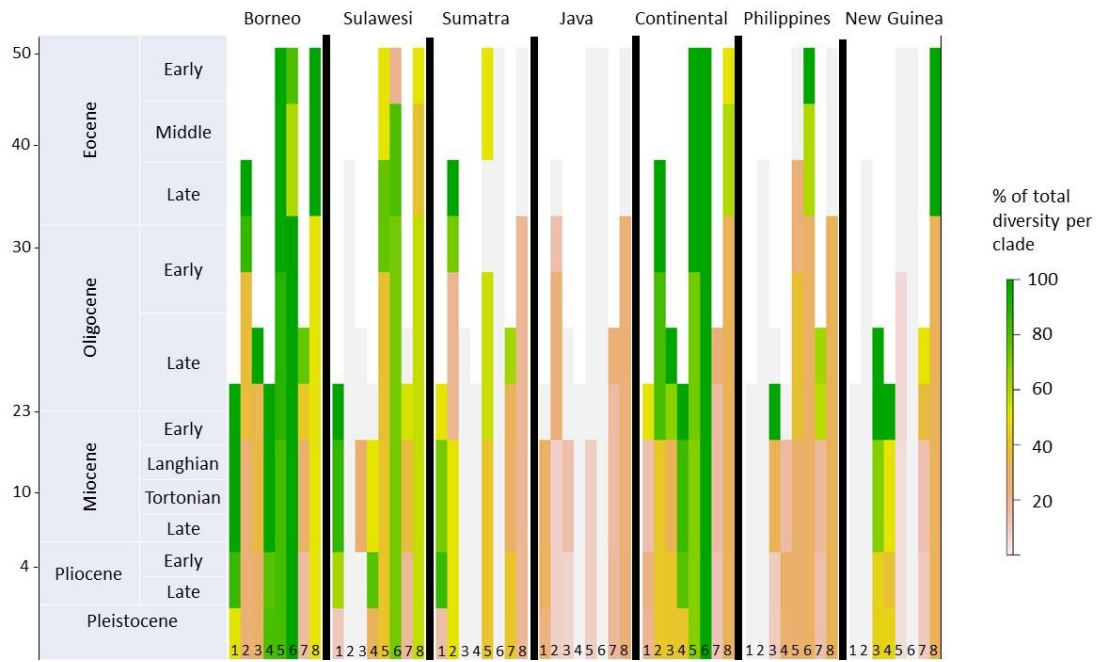
812



814

815 Figure S25. Reconstructed species richness over time across the Indo-Australian
 816 Archipelago under low rates of extinction scenario for eight taxonomic groups. 1:
 817 Crabs, 2: Parachuting frogs, 3: *Pseuduvaria* treelets, 4: Orchids, 5: Breadfruit, 6:
 818 Taros, 7: *Cyrtandra* herbs, 8: Crickets. Colour code shows the relative number of
 819 species inhabiting each location at each time point. Notice that widespread
 820 ancestors contribute to the species richness of several locations. Time scale on the
 821 left is in million years.

822



823

824 Figure S26. Reconstructed species richness over time across the Indo-Australian
 825 Archipelago under high rates of extinction scenario for eight taxonomic groups. 1:
 826 Crabs, 2: Parachuting frogs, 3: *Pseuduvaria* treelets, 4: Orchids, 5: Breadfruit, 6:
 827 Taros, 7: *Cyrtandra* herbs, 8: Crickets. Colour code shows the relative number of
 828 species inhabiting each location at each time point. Notice that widespread
 829 ancestors contribute to the species richness of several locations. Time scale on the
 830 left is in million years.

831

832

833